



## Article

# A System Dynamics Model to Facilitate the Development of Policy for Urban Heat Island Mitigation

Robert Dare

School of Urban Planning, McGill University, Macdonald-Harrington Building (Suite 400), 815 Sherbrooke Street West, Montreal, QC H3A 0C2, Canada; robert\_dare@me.com

**Abstract:** This article presents a customized system dynamics model to facilitate the informed development of policy for urban heat island mitigation within the context of future climate change, and with special emphasis on the reduction of heat-related mortality. The model incorporates a variety of components (incl.: the urban heat island effect; population dynamics; climate change impacts on temperature; and heat-related mortality) and is intended to provide urban planning and related professionals with: a facilitated means of understanding the risk of heat-related mortality within the urban heat island; and location-specific information to support the development of reasoned and targeted urban heat island mitigation policy.

**Keywords:** system dynamics model; urban heat island; heat-related mortality; climate change; mitigation; land use; policy development



**Citation:** Dare, R. A System Dynamics Model to Facilitate the Development of Policy for Urban Heat Island Mitigation. *Urban Sci.* **2021**, *5*, 19. <https://doi.org/10.3390/urbansci5010019>

Received: 30 November 2020  
Accepted: 21 January 2021  
Published: 1 February 2021

**Publisher's Note:** MDPI stays neutral with regard to jurisdictional claims in published maps and institutional affiliations.



**Copyright:** © 2021 by the author. Licensee MDPI, Basel, Switzerland. This article is an open access article distributed under the terms and conditions of the Creative Commons Attribution (CC BY) license (<https://creativecommons.org/licenses/by/4.0/>).

## 1. Introduction

Heat is a serious public health threat that results in a significant amount of mortality on an annual basis. To illustrate, Kalkstein et al. [1] have estimated that there was an annual average of approximately 1300 heat-related deaths in 40 major American cities over the 30-year period from 1975 through 2004. Similarly, Cheng et al. [2] have estimated that, over the 47-year period from 1954 through 2000, there was an annual average of approximately 320 heat-related deaths in the Canadian cities of Toronto, Montreal, Ottawa and Windsor. Additionally, Guest et al. [3] have estimated that there was an annual average of 175 heat-related deaths in the Australian cities of Adelaide, Brisbane, Melbourne, Perth and Sydney over the period from 1979 through 1990. Annual average estimates of heat-related deaths can, however, be exceeded during brief periods of extreme heat (i.e., heatwaves). This is demonstrated by the example of a heatwave in the central part of the United States that resulted in an estimated total of approximately 525 excess deaths over a five-day period in July 1995 in Chicago alone [4], where, according to Kalkstein et al. [1], there was an annual average of approximately 93 heat-related deaths from 1975 through 2004. Other such examples of heatwaves with significant mortality abound (see: [5–8]).

Based on the above, it is clear that heat is a serious public health threat when considered in a historical context. However, heat is even more troubling when considered in a future context. Indeed, with recent climate models projecting an increase of up to 4.8 °C in the global mean surface temperature and an overall increase in the frequency and duration of extreme heat events through 2100 [9], it is clear that extreme heat will pose an increased public health threat in the years to come. This threat will be further exacerbated by the fact that populations are growing older in many world regions (see: [10]). Indeed, the elderly are among the most impacted by the public health threat of heat [11–17]. Growth in elderly populations will, therefore, contribute to the increased significance of the public health threat of heat.

Claims that extreme heat will pose an increased public health threat in the years to come are further supported by a significant body of research that indicates that heat-related mortality will rise sharply in the future (see: [18–23]). Although heat-related mortality can

be expected to increase, humans have a natural ability to acclimatize to high temperatures through physiological processes and behavior modification (e.g., reducing activity levels and using air conditioning), which is frequently unaccounted for in projections of heat-related mortality. The fact that acclimatization effects are frequently unaccounted for in projections of heat-related mortality is demonstrated by a comparison of 14 projections by Huang et al. [24], which indicated that only half of the projections had accounted for, or examined, acclimatization to higher temperatures. Thus, one may conclude that projections of heat-related mortality are frequently overstated. Nevertheless, heat will continue to be a serious public health threat.

As demonstrated by multiple, historic studies of excess deaths related to extreme heat exposure (see: [4,7,8,25]), the public health threat of heat is particularly severe in urban areas. The presence of the urban heat island effect is a key explanation for this increased threat. Indeed, this phenomenon causes urban areas to be considerably warmer than surrounding rural areas and, therewith, increases the vulnerability of urban populations to heat-related mortality [26,27]. To illustrate, the heightened vulnerability of urban populations to the public health threat of heat is evident in the fact that about 91 percent of the excess deaths that occurred in France during an August 2003 heatwave occurred in urban areas with at least 5000 residents [25].

Despite its significant impact on heat-related mortality, there is great potential to mitigate the urban heat island effect at the local level. The basis for this claim lies in the fact that the urban heat island effect is principally the result of the impacts of the built environment on surface energy balance [27]. Within individual urban heat islands, wide temperature variations that correspond with different land uses, and types of land surface cover, demonstrate the impacts of the built environment on surface energy balance (see: [27–29]). Indeed, Martin et al. [29] have observed differences in land surface temperature, which is closely correlated with ambient temperature (i.e., air temperature; see: [29–31]), of up to approximately 16 °C in Montreal, with the warmest and coolest areas of the city being located in industrial and vegetated areas, respectively; they note that the different thermal capacities of impervious surfaces, soils, vegetation and water to absorb and emit heat impact the formation of urban heat islands.

The local level is well aware of the urban heat island effect and the potential for its mitigation. To illustrate, as has been demonstrated in Dare [32], the ten most populous municipalities in both the United States and Canada have been found to have a combined total of 307 unique instances of direct policy measures for urban heat island mitigation, with 85.7 percent of which prescribing approaches aimed at augmentation of latent heat flux, provision of shade, and increasing of surface albedo (n.b., the remaining 14.3 percent do not prescribe an approach). For as aware of the urban heat island effect and the potential for its mitigation as the local level is, however, there appears to be a lack of awareness of the public health impacts of the urban heat island effect. Indeed, of the aforementioned 307 unique instances of direct policy measures, only about 13.4 percent are framed in relation to public health.

Given the lack of awareness of the public health impacts of the urban heat island effect and the prospect of increased heat-related mortality in the future, it is important to foster and support local efforts for urban heat island mitigation in order to reduce the potential for heat-related mortality. To this end, this article presents a system dynamics model, which is referred to herein as the *Urban Heat Island Mitigation Planning Tool* (UHIMPT model) and may be used to facilitate an improved understanding of the public health threat of heat within the urban heat island and, therewith, the informed development of policy for its mitigation. To promote the future use and application of the UHIMPT model at the local level, this article pays particular attention to its structure and parameterization. In doing so, the intent is to provide urban planning and related professionals with sufficient information to customize and apply the UHIMPT model in a given location.

### Article Organization

The remainder of this article is structured as follows:

- **Section 2. Materials and Methods** provides: an overview description of the *UHIMPT* model (incl., its components, required data inputs and data outputs), and a thorough review of its mathematical parameterization (incl., the presentation of each equation);
- **Section 3. Results** provides an illustrative demonstration of how the *UHIMPT* model may be customized and used to facilitate an improved understanding of the public health threat of heat within the urban heat island and, therewith, the informed development of policy for its mitigation within a given location;
- **Section 4. Discussion** reviews: the results of the illustrative demonstration of the *UHIMPT* model, and the demonstrated utility of the *UHIMPT* model;
- **Section 5. Model Validation** applies common structural and behavioral validation tests to the *UHIMPT* model in order to verify that: the model structure represents actual conditions accurately and in sufficient detail, and simulated behavior reasonably mimics observed behavior to a degree that is sufficient to instill confidence;
- **Section 6. Model Limitations** provides a discussion of the various limitations of the *UHIMPT* model and, where relevant, identifies potential means to overcome same;
- **Section 7. Proper Model Use** explores, in consideration of model structure and limitations, how the *UHIMPT* model should, and should not, be used;
- **Section 8. Conclusion** summarizes the utility of the *UHIMPT* model.

## 2. Materials and Methods

### 2.1. Model Description

The *UHIMPT* model is a system dynamics model, which was created with Release 10.0 of the *Systems Thinking, Experimental Learning Laboratory with Animation* (STELLA) structural equation modeling software package by isee systems, Inc. of Lebanon, NH, USA (n.b., though STELLA was used in this instance, the *UHIMPT* model is presented in such a way that it may be recreated in other programming languages with other software packages). It is intended to be adaptable and easily applied in a variety of study areas and operates on an annual time step in order to simulate conditions during the warmest month (i.e., when the risk of heat-related mortality is greatest).

The *UHIMPT* model includes a variety of components (incl.: urban heat island effect; population dynamics; climate change impacts on temperature; and heat-related mortality) and provides the user with the opportunity to estimate the impacts of various hypothetical urban heat island mitigation strategies on heat-related mortality. Complete information on the various components of the *UHIMPT* model, as well as required data inputs and model outputs, is provided in Sections 2.1.1–2.1.3.

#### 2.1.1. Components

The individual components of the *UHIMPT* model, as well as the relationships between them, are discussed in the following subsections.

Please note that the purpose of Section 2.1.1 is to explain the general function of the model, and the generalized interactions among the individual components thereof. Data requirements of each component are discussed in Section 2.1.2. Parameterization of each component is discussed in Section 2.2.

#### Urban Heat Island

The *UHIMPT* model accounts for the urban heat island effect. While there are numerous conceptions of the urban heat island in the literature (see: [27]), the surface urban heat island and the canopy layer urban heat island are of primary interest in this discussion. The surface urban heat island is determined by the temperature of the land surface, which is influenced by all urban features (e.g., paved surfaces, vegetation, walls, roofs, building shadows), and exhibits the highest amplitude (i.e., urban–rural temperature difference) during the daytime when solar heating creates the largest differences between pervious

and impervious surfaces (see: [27]). The canopy layer urban heat island, on the other hand, is measured by air temperature below the tops of buildings and trees (i.e., within the urban canopy) and generally exhibits the highest amplitude at night because urban areas typically retain heat longer than rural areas and, thus, cool more slowly (see: [27,33]).

The *UHIMPT* model examines canopy layer urban heat island. However, it does not do so by a typical means of analysis (e.g., mobile transect measurement of air temperature as in Oke [34]) or based on nighttime temperatures. Indeed, the *UHIMPT* model's accounting of the urban heat island effect relies upon user-input data on normal (i.e., derived from climate norms) urban heat island amplitude during the warmest month, as measured by air temperature and specifically representing: the difference between observed mean warmest month air temperatures averaged over the entirety of the urban and the rural (i.e., surrounding) areas, and the difference between the mean maximum warmest month air temperatures in the urban and rural areas. This results in the incorporation of baseline measures of both the normal mean warmest month urban heat island amplitude, and the normal mean maximum warmest month urban heat island amplitude (Note 1), within the *UHIMPT* model. The *UHIMPT* model relies upon such measurements of urban heat island amplitude because of the widespread availability of appropriate data, which is discussed in Section 2.1.2 and eliminates the need to perform specialized data collection and analysis (e.g., mobile transect measurement of air temperature as in Oke [34]; Note 2). This, in turn, facilitates the application of the *UHIMPT* model.

It is important to note that urban heat island amplitude is not static. As cities grow and develop, urban heat island amplitude, under conventional development scenarios and without mitigation efforts, has shown a tendency to increase. This is demonstrated in the case of the planned community of Columbia, Maryland, where Landsberg [35] documented an increase of 6 °C in urban heat island amplitude between 1968 and 1974, when the town was in the early stages of development and grew in population from approximately 1000 residents in 1968 to slightly more than 20,000 residents in 1974. Other examples of growth and dynamism in urban heat island amplitude abound (see: [36–38]).

The development of the urban heat island effect has frequently been explained as: a function of population growth (see: [34,39–41]), and as a function of the level of development in an area, as measured by sky view factor, which is the proportion of sky that is visible from a given location (see: [42–44]). While both functions may serve as a proxy to simulate the dynamic nature of urban heat island amplitude, the *UHIMPT* model uses population size to do so. Specifically, it adapts the population size–urban heat island amplitude function for North American settlements of Oke [34] to estimate future amplitude based on: projected population size; and the factor of change in amplitude between two consecutive time steps (i.e., years) that is reflected by said function (Notes 3–5). Complete details of the adaptation of Oke's population size–urban heat island amplitude function for use in the *UHIMPT* model are provided in Section 2.2 (Notes 6–7).

The *UHIMPT* model also provides a means of testing the impacts of sundry hypothetical policies for urban heat island mitigation. As shown in Dare [32], urban heat island mitigation policy most frequently prescribes approaches aimed at: augmentation of latent heat flux (e.g., by minimizing impervious surface cover); provision of shade (e.g., by increasing tree canopy); and increasing surface albedo (e.g., by setting performance standards for flat and low-slope roof surfaces). To simulate the impacts of such policies, the *UHIMPT* model includes an adaption of a customized multiple linear regression model, which, as discussed in Section 2.1.2, is developed with user-input data and provides users with the ability to modify land surface temperature by altering: surface albedo; impervious surface cover; and the proportion of vegetation. To render this simulation of the impact of sundry hypothetical policies for urban heat island mitigation compatible with the *UHIMPT* model's examination of the canopy layer urban heat island, the change in land surface temperature is converted to air temperature by means of the linear regression model of Gallo et al. [30], which is discussed in Section 2.2.

To summarize, the *UHIMPT* model accounts for the following aspects of the urban heat island effect:

- Normal mean warmest month urban heat island amplitude;
- Normal mean maximum warmest month urban heat island amplitude;
- Development of the urban heat island effect, as determined by an adapted population size–urban heat island amplitude function for North American settlements;
- Impact of sundry hypothetical policies for urban heat island mitigation.

#### Climate Change Impacts

The *UHIMPT* model accounts for the impacts of climate change on air temperature. To do so, and as described in Section 2.1.2, it requires data on climate norms and projections for the urban and rural areas. With such data, the *UHIMPT* model linearly interpolates the projected impacts of climate change on mean warmest month and mean maximum warmest month air temperature in the urban and rural areas for every time step (i.e., year) and, therewith, the change in urban heat island amplitude resulting from climate change (Note 8). The *UHIMPT* model then uses information from its accounting of the urban heat island effect to estimate overall air temperature of the urban area, as impacted by: climate change; the dynamic nature of urban heat island amplitude; and hypothetical policies for urban heat island mitigation. This calculation of climate change impacts provides input to the calculation of heat-related mortality, which is discussed later in this section.

It is important to note that the *UHIMPT* model itself does not project mean warmest month air temperature and mean maximum warmest month air temperature. As a result, the model does not simulate conditions beyond the last period that is reflected in the user-input projections of mean and mean maximum warmest month air temperatures.

To summarize, the *UHIMPT* model accounts for the following aspects of climate change impacts:

- Normal mean warmest month air temperature;
- Normal mean maximum warmest month air temperature;
- Projected mean warmest month air temperature;
- Projected mean maximum warmest month air temperature;
- Impact of projected temperatures on urban heat island amplitude.

#### Population Dynamics

The *UHIMPT* model includes a cohort-component population projection. The cohort-component population projection methodology is covered extensively in urban planning and related literature (see: [45–49]) and is generally recognized as the most widely used methodology for sub-national population projections (see: [45,47,49]). It accounts for fertility, all-cause mortality and net migration, and is noted for its use in projecting not only population size, but also population structure (e.g., age and sex cohorts).

Although cohort-component population projections most frequently include projections of age and sex cohorts, the *UHIMPT* model incorporates a simplified cohort-component population projection that includes only population size and age cohorts (n.b., the *UHIMPT* model uses single-year age cohorts to make the cohort population projection compatible with its annual time step). It does not include sex cohorts. The reason for this simplification is that the cohort-component population projection is only used by the *UHIMPT* model: to estimate the number of excess deaths that would result from one day of exposure to extreme heat in the urban area (n.b., the risk of heat-related mortality is highest on the day of exposure [50]), as determined by all-cause mortality and the increased relative risk of same that results from exposure to heat, the calculation of which is discussed in the next subsection and relies upon aggregate data that does not distinguish between sexes (Note 9); and to calculate change in urban heat island amplitude, which, as previously discussed, is calculated as a function of total population size. The cohort-component population projection of the *UHIMPT* model is used for no other purposes.

In addition to the above, it is noted that the *UHIMPT* model's cohort-component population projection does not extrapolate or project future trends in mortality, fertility and net migration rates. Instead, the mortality, fertility and net migration rates that are experienced between the past two official censuses are estimated, annualized, and applied in the projection. This simplification has been made in order to reduce user-input data requirements. It has also been made because, as noted by Smith et al. [47]: there is a lack of scientific reasoning that proves that such rates can be accurately projected, particularly in small areas (e.g., a municipality), on the basis of historic information; and the performance of past projections of such rates has generally left much to be desired. It is further noted that the application of static mortality, fertility and net migration rates within the *UHIMPT* model is justified by common practice [46,47,51,52].

To summarize, the *UHIMPT* model analyzes population dynamics with a cohort-component population projection, which accounts for:

- Fertility;
- All-cause mortality;
- Net migration.

#### Heat-Related Mortality

The *UHIMPT* model accounts for heat-related mortality. To do so, it uses the temperature–mortality functions of Nordio et al. [50], which are based on a statistical analysis of more than 42 million death records from –out the contiguous United States and provide regional climate-specific factors of relative risk of mortality resulting from one day of exposure to extreme heat in the urban area (n.b., continental United States-specific the temperature–mortality functions of Nordio et al. [50] may be substituted when the *UHIMPT* model is to be adapted for use in other regions). Specifically, these factors are used, along with the cohort-component population projection and the interpolated projections of air temperature that have been previously described, to estimate the impact of one day of exposure to extreme heat, as represented by mean maximum warmest month air temperature, in the urban area. The appropriate relative risk factor for a given study area is determined by the normal mean summer and winter air temperatures in the region (Note 10).

It is important to note that although humidity has an impact on heat-related mortality, air temperature is a much stronger predictor of same [53,54]. For this reason, and in an effort to simplify the *UHIMPT* model, it relies entirely upon air temperature as a predictor of heat-related mortality. Nonetheless, the temperature–mortality functions of Nordio et al. [50] have been developed with the benefit of a cluster analysis, which identified eight climate clusters covering the continental United States based on relative humidity, mean summer and winter air temperature, and the standard deviation of mean summer and winter air temperature. For each of these climate clusters, Nordio et al. [50] prepared customized temperature–mortality functions, all of which have been incorporated into the *UHIMPT* model (n.b., as explained in Sections 2.1.2 and 2.2.4, the appropriate temperature–mortality function is automatically selected based on user-input data on normal mean summer and winter air temperatures for the region). Thus, although the *UHIMPT* model does not directly rely upon information on relative humidity to explain heat-related mortality, the influence of relative humidity is captured in the temperature–mortality functions of Nordio et al. [50].

In addition to the above, it is noted that a reduction factor is applied to the appropriate factor of relative risk of mortality in order to account for the natural human ability for acclimatization to higher air temperatures resulting from future climate change. This reduction factor is derived from and corresponds with a meta-regression analysis by Nordio et al. [50], which indicates that every 5 °C increase in mean air temperature is accompanied by a 1.78-percent reduction in heat-related mortality (95-Percent CI: 0.82, 2.74).

It is important to note that the *UHIMPT* model does not simply apply a variable relative risk factor that corresponds with projected mean warmest month and coldest month air temperatures for the region at a given time step. Such an approach assumes sudden

acclimatization. Acclimatization, however, is more likely to be gradual and continuous (see: [50,55]). Such a gradual and continuous pattern of acclimatization is captured by applying the aforementioned reduction factor.

Please note that heat-related mortality is calculated for scenarios that assume both no mitigation of the urban heat island effect and mitigation of the urban heat island effect.

To summarize, the *UHIMPT* model accounts for the following aspects of heat-related mortality:

- Impact of mean warmest month air temperature on mortality (i.e., heat-related mortality);
- Impact of mean maximum warmest month air temperature on mortality (i.e., heat-related mortality);
- Impact of acclimatization to higher temperatures resulting from future climate change on heat-related mortality.

#### Summary of Relationships between Model Components

As has been shown by the foregoing discussion, the *UHIMPT* model includes various components to account for the urban heat island effect (incl., the impact of hypothetical urban heat island mitigation policy), the impacts of climate change, population dynamics, and heat-related mortality. The generalized relationships between these components are demonstrated in Figure 1.

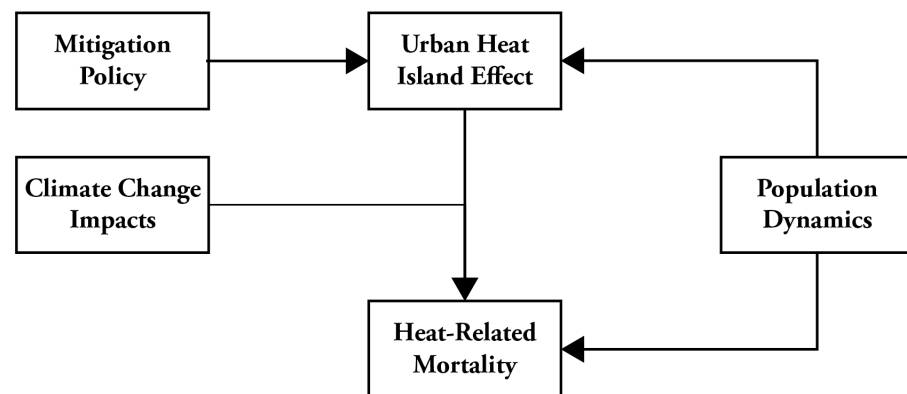


**Figure 1.** Generalized Relationships between *UHIMPT* Model Components.

The generalized relationships between components of the *UHIMPT* model are shown in Figure 1. As shown, the accounting of the urban heat island effect and climate change impacts collectively impact the accounting of heat-related mortality. Specifically, the accountings of the urban heat island effect and climate change impacts are used to obtain an estimate of overall mean warmest month and mean maximum warmest month air temperature in the urban area, which is then used to determine the relative risk of heat-related mortality. As represented in the *UHIMPT* model, climate change impacts further impact the accounting of heat-related mortality in that projected increases in mean air temperature result in reduced relative risk of heat-related mortality. In addition, heat-related mortality is further impacted by population dynamics. Indeed, it uses the cohort-component population projection, and specifically the cohort-specific population totals and mortality rates, in the estimation of the impacts of one day of exposure to extreme heat. In addition, population dynamics impact the accounting of the urban heat island effect. Specifically, the *UHIMPT* model uses population growth represented in the cohort-component population projection as a proxy for increased urban heat island amplitude resulting from urban growth and development. Finally, it is noted that hypothetical urban heat island mitigation policy alters the magnitude of the urban heat island effect and, in turn, the accounting of heat-related mortality.

### 2.1.2. Data Inputs

The *UHIMPT* model has moderate data input requirements, which include data on climate norms and projections, baseline population data, and sundry geospatial datasets (e.g., geographic boundaries, impervious cover). This section provides an overview of the data input requirements for each of its individual components. In addition, Supplement A provides an inventory of data input requirements and potential data sources in tabular format.

#### Urban Heat Island

The accounting of the urban heat island effect requires the following data: normal mean warmest month air temperature for the urban and rural (i.e., surrounding) areas; and the normal mean maximum warmest month air temperature for the same areas. These data may be obtained from a raster-based geospatial dataset, which is presented in Wang et al. [56] and has a spatial resolution of 1.0 km<sup>2</sup>. Said dataset provides coverage for all regions of North America (Note 11).

As previously explained in Section 2.1.1, the *UHIMPT* model uses a customized multiple linear regression model to demonstrate the relationship of surface albedo, impervious cover and the proportion of vegetation with land surface temperature. This multiple linear regression model relies on user-input data and must be tailored by the user to the specific geographic area of application of the *UHIMPT* model. To do so, the following data are required: recent cloud-free, daytime Landsat 8 satellite imagery that was captured in the warmest month, or other such satellite imagery of the same or higher resolution that has ultra-blue, green, red, near infrared, and thermal infrared bands; and a vector-based geospatial dataset representing impervious cover (n.b., such datasets are typically derived from remote sensing methodologies and frequently published by state, regional and local governments on public geospatial data clearinghouse platforms). The multiple linear regression model is further discussed in Sections 2.2 and 5, as well as in Supplement B.

#### Climate Change Impacts

The *UHIMPT* model's accounting of climate change impacts requires the following data for the urban and rural areas: normal mean warmest month air temperature; projected mean warmest month air temperature for three periods (e.g., 2020's, 2050's, 2080's), as downscaled to the area of interest; normal mean maximum warmest month air temperature; projected mean maximum warmest month air temperature for three periods, as downscaled to the area of interest and for the same points as provided for mean warmest month air temperature; and the first and last years of the periods that are represented in the projected mean warmest month and mean maximum air temperatures. All other required information is derived from data inputs to other components. This component (i.e., climate change impacts) has no further data input requirements.

There are a variety of sources for information on climate norms and projections. The most important criterion for use in the *UHIMPT* model is that the data are of a spatial resolution that is high enough to represent local conditions (n.b. it is recommended that the spatial resolution be no less than 1.0 km<sup>2</sup>). An example of a suitable source for information on climate norms and projections is the geospatial dataset that is presented in Wang et al. [56]. This dataset, which covers all regions of North America at a spatial resolution of 1.0 km<sup>2</sup>, provides climate norms for the period from 1981 through 2010, and projections for the following periods: 2020s, which is calculated as an average from 2011 through 2040; 2050s, which is calculated as an average from 2041 through 2070; and 2080s, which is calculated as an average from 2071 through 2100.

#### Population Dynamics

The following data are required to prepare the *UHIMPT* model's cohort-component population projection: total population by single-year of age as reported in the past two official censuses; total births by single-year of age of the parous female for the period

between the past two censuses; and total deaths by single-year of age of decedent for the period between the past two censuses. Information on population by age can be obtained from official census agencies (e.g., United States Census Bureau; Statistics Canada). Information on births and deaths can be obtained from local or regional health departments, or offices of vital statistics.

#### Heat-Related Mortality

As previously noted, the calculation of heat-related mortality relies upon the temperature–mortality functions of Nordio et al. [50], which are programmed into the *UHIMPT* model. The following data are required to enable the selection of the proper temperature–mortality function: normal mean summer air temperature for the region (i.e., urban and rural areas combined); and normal mean winter air temperature for the region. The geospatial dataset of Wang et al. [56] is a known source of this data.

In addition, a temperature rise–acclimatization change factor that is provided in Nordio et al. [50] is used to account for the natural human ability to acclimatize to higher temperatures. This change factor is programmed into the *UHIMPT* model. However, data on projected mean annual air temperature for three periods, as downscaled to the region (i.e., urban and rural areas combined) and for the same periods as provided for the accounting of climate change impacts is required. The aforementioned geospatial dataset of Wang et al. [56] is an example of a known source for these data. All other required information is derived from other components. This component has no further data input requirements.

#### Other Data Requirements

In addition to the data requirements that have been identified in the preceding discussion, vector-based geospatial datasets representing the boundaries of the urban area (e.g., municipal boundary) and the broader region (e.g.: core-based statistical areas; census metropolitan area; an appropriate buffer of the urban area) are needed to make full use of satellite imagery and select data from Wang et al. [56] for processing and use in the *UHIMPT* model.

#### 2.1.3. Model Outputs

The *UHIMPT* model provides the user with information about:

- Future urban heat island amplitude, as measured by urban–rural differences in mean warmest month and mean maximum warmest month temperatures and impacted by climate change and the dynamic nature of urban heat island amplitude, but not hypothetical policies for urban heat island mitigation;
- Future urban heat island amplitude, as measured by urban–rural differences in mean warmest month and mean maximum warmest month temperatures and impacted by climate change and the dynamic nature of urban heat island amplitude, as well as hypothetical policies for urban heat island mitigation;
- The impacts of heat-related mortality in the urban area, as expressed as the number of deaths that can be expected to result from one day of exposure to the mean warmest month and mean maximum warmest month temperatures for both a no-mitigation and urban heat island mitigation scenarios, but not accounting for the impacts of the human capacity for acclimatization to higher temperatures;
- The impacts of heat-related mortality in the urban area, as expressed as the number of deaths that can be expected to result from one day of exposure to mean warmest month temperature and mean maximum warmest month temperature for both no-mitigation and urban heat island mitigation scenarios with accounting for the impacts of the human capacity for acclimatization to higher temperatures.

## 2.2. Model Parameterization

This section provides details of the mathematical parameterization of the *UHIMPT* model. Please note that although the *UHIMPT* model was developed in STELLA, the information provided herein facilitates the replication of the *UHIMPT* model in a variety of other software packages and programming languages.

### 2.2.1. Urban Heat Island

Baseline measures of normal mean urban heat island amplitude and normal mean maximum urban heat island amplitude are the starting point of the parameterization of this component. Normal mean warmest month urban heat island amplitude is calculated by subtracting the normal mean warmest month air temperature of the rural (i.e., surrounding) area from that of the urban area. Similarly, normal mean maximum warmest month urban heat island amplitude is calculated by subtracting the normal mean maximum warmest month air temperature of the rural area from that of the urban area. These operations are summarized in Equations (1) and (2).

Equation for Normal Mean Warmest Month Urban Heat Island Amplitude:

$$\bar{A}_{Baseline, Normal_{Warmest\ Month}} = \bar{T}_{Normal_{Warmest\ Month}, Urban} - \bar{T}_{Normal_{Warmest\ Month}, Rural}. \quad (1)$$

Equation for Normal Mean Maximum Warmest Month Urban Heat Island Amplitude:

$$\bar{A}_{Baseline, Maximum_{Warmest\ Month}} = \bar{T}_{Maximum_{Warmest\ Month}, Urban} - \bar{T}_{Maximum_{Warmest\ Month}, Rural}. \quad (2)$$

In Equations (1) and (2),  $\bar{A}$  represents mean urban heat island amplitude and  $\bar{T}$  represents mean air temperature. Subscripts associated with these variables specify magnitudinal (e.g., normal, maximum), locational (e.g., urban, rural) and temporal (e.g., baseline, warmest month) characteristics such that:  $\bar{A}_{Baseline, Normal_{Warmest\ Month}}$  represents the normal mean urban heat island amplitude in the warmest month; and  $\bar{T}_{Maximum_{Warmest\ Month}, Urban}$  represents normal mean maximum air temperature in the urban area during the warmest month.

As has been noted in Section 2.1, urban heat island amplitude is not static. To account for this fact, the *UHIMPT* model adapts the population size–urban heat island amplitude function for North American settlements of Oke [34] to estimate future amplitude. Specifically, the total populations of two consecutive time steps are applied to Oke's [34] population size–urban heat island amplitude function in order to calculate a factor of change in urban heat island amplitude between the same time steps. This factor of change is then applied to the actual urban heat island amplitude of the previous (e.g., first) time step in order to yield an estimate of urban heat island amplitude in the current (e.g., second) time step. In cases where a population decline is projected between time steps, there is assumed to be no change in urban heat island amplitude; this is based on the assumption that there would be a significant lag between population decline and potential resulting modifications of the built environment (e.g., demolition of unused structures, renaturation), which would yield a reduction of urban heat island amplitude. Calculation of change in urban heat island amplitude is demonstrated in Equations (3) and (4), which are applied between each pair of consecutive time steps in order to yield calculations of mean warmest month and mean maximum warmest month urban heat island amplitudes (Note 12).

Equation for Mean Warmest Month Urban Heat Island Amplitude:

$$\bar{A}_{x_{\text{Warmest Month}}} = \begin{cases} \left( \left( \left( \left( \frac{2.96 \times \log\left(\left(\sum_{i=\text{Cohort 1}}^{\text{Last Cohort}} P_x\right) - 6.41\right)}{\left(\sum_{i=\text{Cohort 1}}^{\text{Last Cohort}} P_{x-1}\right) - 6.41\right)} + 1 \right) \right) \right) \times \bar{A}_{x-1_{\text{Warmest Month}}}, & \text{if } \Delta P > 0 \\ \bar{A}_{x-1_{\text{Warmest Month}}}, & \text{if } \Delta P \leq 0. \end{cases} \quad (3)$$

Equation for Mean Maximum Warmest Month Urban Heat Island Amplitude:

$$\bar{A}_{x, \text{Maximum Warmest Month}} = \begin{cases} \left( \left( \left( \left( \frac{2.96 \times \log\left(\left(\sum_{i=\text{Cohort 1}}^{\text{Last Cohort}} P_x\right) - 6.41\right)}{\left(\sum_{i=\text{Cohort 1}}^{\text{Last Cohort}} P_{x-1}\right) - 6.41\right)} + 1 \right) \right) \right) \times \bar{A}_{x-1, \text{Maximum Warmest Month}}, & \text{if } \Delta P > 0 \\ \bar{A}_{x-1, \text{Maximum Warmest Month}}, & \text{if } \Delta P \leq 0. \end{cases} \quad (4)$$

In Equations (3) and (4),  $\bar{A}$  represents mean urban heat island amplitude and  $P$  represents population, the calculation of which is described in Section 2.2.3. The subscript  $x$  represents the current step. The subscript  $x - 1$  represents the previous time step, or the baseline (i.e.,  $\bar{A}_{\text{Baseline, Normal Warmest Month}}$  or  $\bar{A}_{\text{Baseline, Maximum Warmest Month}}$ , as appropriate and represented in Equations (1) and (2), respectively) when the current time step (i.e.,  $x$ ) is the first time step. All other subscripts are as in Equations (1) and (2).

The UHIMPT model provides users with the ability to estimate the impacts of various hypothetical urban heat island mitigation strategies. Specifically, it enables users to simulate the impacts of changes in mean surface albedo, the mean proportion of impervious surface cover and the mean proportion of vegetation on air temperature. This is achieved by incorporating: the standard (i.e., beta [ $\beta$ ]) coefficients of a customized multiple linear regression model wherein the surface albedo and proportions of impervious surface cover and vegetation in a given area are the independent variables and land surface temperature of the same area is the dependent variable (Note 13); and the linear regression model of Gallo et al. [30], which provides a means of estimating air temperature from land surface temperature, in order to convert the simulated impacts of alterations of surface albedo, impervious surface cover and the proportion of vegetation on land surface temperature to air temperature (Note 14). Equations (5) and (6) are used to calculate modification of mean and mean maximum warmest month urban heat island amplitudes, respectively.

Equation for Modification of Mean Warmest Month Urban Heat Island Amplitude:

$$\bar{A}_{x_{\text{Warmest Month}}} + \left( \left( \frac{\bar{A}_{x_{\text{Warmest Month, Modified}}} - \left( \left( \frac{(\beta_i \times \Delta \bar{I}) - (\beta_v \times \Delta \bar{V}) - (\beta_a \times \Delta \bar{\alpha}) - 2.82}{1.15} \right) \right)}{1.15} \right) + 2.452 \right). \quad (5)$$

Equation for Modification of Mean Maximum Warmest Month Urban Heat Island Amplitude:

$$\bar{A}_{x, \text{Maximum Warmest Month}} + \left( \left( \frac{\bar{A}_{x, \text{Maximum Warmest Month, Modified}}} - \left( \left( \frac{(\beta_i \times \Delta \bar{I}) - (\beta_v \times \Delta \bar{V}) - (\beta_a \times \Delta \bar{\alpha}) - 2.82}{1.15} \right) \right) \right) + 2.452 \right). \quad (6)$$

In Equations (5) and (6):  $\bar{A}$  represents mean urban heat island amplitude;  $\Delta \bar{I}$  represents the change in mean proportion of impervious surface cover in the urban area (Note 15);  $\Delta \bar{V}$  represents the change in mean proportion of vegetation in the urban area (Note 16);  $\Delta \bar{\alpha}$

represents the change in mean surface albedo in the urban area (Note 17);  $\beta_i$  represents the standard (i.e., beta [ $\beta$ ]) coefficient for proportion of impervious surface cover that results when the surface albedo and proportions of impervious surface cover and vegetation of a given area are regressed on its land surface temperature;  $\beta_v$  represents the standard (i.e., beta [ $\beta$ ]) coefficient for proportion of vegetation that results when the surface albedo and proportions of impervious surface cover and vegetation of a given area are regressed on its land surface temperature; and  $\beta_\alpha$  represents the standard (i.e., beta [ $\beta$ ]) coefficient for albedo that results when the surface albedo and proportions of impervious surface cover and vegetation of a given area are regressed on its land surface temperature. Subscripts, other than those contained in standard (i.e., beta [ $\beta$ ]) coefficients, are as in Equations (1)–(4), except that the subscript *Modified* denotes the modified urban heat island amplitude.

Please note that Section 3.1 provides an illustrative model demonstration that includes details on the preparation of a multiple linear regression model for use in the *UHIMPT* model.

### 2.2.2. Climate Change Impacts

The first step in the parameterization of climate change impacts is to determine the midpoints of the three periods that are represented in the projections of mean warmest month and mean maximum warmest month air temperatures in the urban and rural areas. This is done by: first subtracting the first year of the period from the final year of the same period; then dividing the resulting difference by two; and lastly, by adding the resulting quotient to the first year of the period. In cases where the result of this set of operations is not a whole number, the number is rounded down to the nearest whole number. The calculation of midpoints of periods is shown in Equation (7).

Equation for Midpoint of Period:

$$M_{Period_x} = \left[ \left( \frac{Y_{Final,Period_x} - Y_{First,Period_x}}{2} \right) + Y_{First,Period_x} \right] \quad (7)$$

In Equation (7),  $M$  represents midpoint and  $Y$  represents year. Subscripts denote final and first years of particular periods. For instance, the subscript in  $Y_{Final, Period_x}$  indicates the final year of a given period. Please note that this equation is applied to each of the three periods that are represented in the projections of mean warmest month and mean maximum warmest month air temperatures in the urban and rural areas.

After midpoints have been calculated, the period-specific projections of mean warmest month air temperature and mean maximum warmest month air temperature are annualized by means of linear interpolation. The first step in the annualization of the projections is to calculate the change in degrees that is reflected between the projected value (i.e., mean warmest month or mean maximum air temperature) and the corresponding value of the previous period, or, in the case of the first period, the value that represents the climate norm. The change in degrees is then divided by the difference, in number of years, between midpoints, or, in the case of the first period, between the midpoint of the first period and the last year that is represented by the climate norm; the result of this operation is the linearly interpolated annual change in air temperature. This change in air temperature is then multiplied by the time step, as represented by the number of years that have elapsed since the last year represented by the climate norm or the midpoint of the previous period, and then added to the corresponding climate norm or linearly interpolated projected value of the midpoint of the previous period, as appropriate, in order to obtain a linearly interpolated projected value for a given year of the next period (Note 18). Equations (8)–(10) detail the annualization of projections for mean warmest month air temperature for the first, second and third projected periods. These equations are followed by Equations (11)–(13), which detail the annualization of projections for mean maximum warmest month air temperature for the projected periods. Please note that Equations (8)–(13) are applied separately to the projections of mean warmest month and mean maximum warmest month air temperatures in the urban and rural areas.

Equation for Annualization of Projections of Mean Warmest Month Air Temperature (First Projected Period):

$$\left( \left( \frac{\bar{T}_{x, Interpolated_{Warmest\ Month, Period_1}} - \bar{T}_{Warmest\ Month, Norm}}{M_{Period_1} - E_{Norm}} \right) \times S_{[E_{Norm+1} \dots M_{Period_1}]} \right) + \bar{T}_{Norm}. \quad (8)$$

Equation for Annualization of Projections of Mean Warmest Month Air Temperature (Second Projected Period):

$$\left( \left( \frac{\bar{T}_{x, Interpolated_{Warmest\ Month, Period_2}} - \bar{T}_{Warmest\ Month, Period_1}}{M_{Period_2} - M_{Period_1}} \right) \times S_{[M_{Period_1+1} \dots E_{Period_2}]} \right) + \bar{T}_{Interpolated_{Warmest\ Month, Period_1, Final\ Year}}. \quad (9)$$

Equation for Annualization of Projections of Mean Warmest Month Air Temperature (Third Projected Period):

$$\left( \left( \frac{\bar{T}_{x, Interpolated_{Warmest\ Month, Period_3}} - \bar{T}_{Warmest\ Month, Period_2}}{M_{Period_3} - M_{Period_2}} \right) \times S_{[M_{Period_2+1} \dots E_{Period_3}]} \right) + \bar{T}_{Interpolated_{Warmest\ Month, Period_2, Final\ Year}}. \quad (10)$$

Equation for Annualization of Projections of Mean Maximum Warmest Month Air Temperature (First Projected Period):

$$\left( \left( \frac{\bar{T}_{x, Interpolated, Maximum_{Warmest\ Month, Period_1}} - \bar{T}_{Maximum_{Warmest\ Month, Norm}}}{M_{Period_1} - E_{Norm}} \right) \times S_{[E_{Norm+1} \dots M_{Period_1}]} \right) + \bar{T}_{Norm}. \quad (11)$$

Equation for Annualization of Projections of Mean Maximum Warmest Month Air Temperature (Second Projected Period):

$$\left( \left( \frac{\bar{T}_{x, Interpolated, Maximum_{Warmest\ Month, Period_2}} - \bar{T}_{Maximum_{Warmest\ Month, Period_1}}}{M_{Period_2} - M_{Period_1}} \right) \times S_{[M_{Period_1+1} \dots M_{Period_2}]} \right) + \bar{T}_{Interpolated, Maximum_{Warmest\ Month, Period_1, Final\ Year}}. \quad (12)$$

Equation for Annualization of Projections of Mean Maximum Warmest Month Air Temperature (Third Projected Period):

$$\left( \left( \frac{\bar{T}_{x, Interpolated, Maximum_{Warmest\ Month, Period_3}} - \bar{T}_{Maximum_{Warmest\ Month, Period_2}}}{M_{Period_3} - M_{Period_2}} \right) \times S_{[M_{Period_2+1} \dots M_{Period_3}]} \right) + \bar{T}_{Interpolated, Maximum_{Warmest\ Month, Period_2, Final\ Year}}. \quad (13)$$

In Equations (8)–(13),  $\bar{T}$  represents mean temperature and  $M$  represents midpoint, as calculated in Equation (7). Subscripts associated with variables  $\bar{T}$  and  $M$  specify characteristics (e.g., interpolated temperature, maximum temperature) and period (e.g., the first projected period, warmest month and, in the case of  $x$ , the current step) such that  $\bar{T}_{x, Interpolated, Maximum_{Warmest\ Month, Period_1}}$  denotes the interpolated mean maximum temperature during the warmest month for a given time step of the first projected period. In addition, it is noted that  $E_{Norm}$  means the last (i.e., end) year represented by the climate norm. The variable  $S$  represents a given time step, as represented by number of years that have elapsed since the last year represented by the climate norm or the first year of the projected period; it is accompanied by the subscript to specify the range of time steps,

such that  $S_{[E_{Norm+1} \dots M_{Period_1}]}$  indicates that the first time step is one year after the last year represented by the climate norm, and the last time step is the midpoint of the first projected period. It is reiterated that Equations (8)–(13) are applied separately to the projections of mean warmest month and mean maximum warmest month air temperatures in the urban and rural areas.

After having annualized the projections of mean warmest month and mean maximum warmest month air temperatures for the urban and rural areas, the projected impacts of climate change on urban heat island amplitude are calculated by: first subtracting the annualized projection of mean warmest month and mean maximum warmest month air temperatures in the rural area from the annualized projection of mean warmest month and mean maximum warmest month air temperatures in the urban area; and then subtracting the normal mean and normal mean maximum warmest month and mean urban heat island amplitudes, as calculated with Equations (1) and (2), respectively, and which are discussed within the context of Section 2.2.1, from the difference between the annualized projections of mean warmest month and mean maximum warmest month air temperatures in the urban and rural areas, as calculated in the previous step. These operations results in the isolation of the projected change over the baseline urban heat island amplitudes that are reflected in the annualized projections of mean warmest month and mean maximum warmest month air temperatures in the urban area. Equations (14) and (15) detail these operations.

Equation for Isolation of Climate Change Impacts on Mean Warmest Month Urban Heat Island Amplitude:

$$\overline{\Delta A}_{x, Interpolated Warmest Month, Period_x} = \overline{T}_{x, Interpolated Warmest Month, Urban, Period_x} - \overline{T}_{x, Interpolated Warmest Month, Rural, Period_x} \quad (14)$$

Equation for Isolation of Climate Change Impacts on Mean Maximum Warmest Month Urban Heat Island Amplitude:

$$\overline{\Delta A}_{x, Interpolated, Maximum Warmest Month, Period_x} = \overline{T}_{x, Interpolated, Maximum Warmest Month, Urban, Period_x} - \overline{T}_{x, Interpolated, Maximum Warmest Month, Rural, Period_x} \quad (15)$$

In Equations (14) and (15),  $\overline{A}$  represents mean urban heat island amplitude. All other notation is as in Equations (8)–(13).

Finally, it is noted that the sum of projected climate change impacts on urban heat island amplitude and the estimated impacts of hypothetical planning interventions on urban heat island amplitude, which are calculated with Equations (5) and (6) of the previous section, represent the estimated total urban heat island amplitude at a given time step, as impacted by both projected climate change, population-based urban heat island dynamics, and hypothetical planning interventions. When this estimate of total urban heat island amplitude is added to the annualized projections of mean warmest month and mean maximum warmest month air temperatures in the rural areas, the calculation of which is demonstrated in this section, the total estimated air temperature of the urban heat island at a given time step is yielded. These operations are demonstrated in Equations (16)–(19).

Equation for Total Mean Warmest Month Urban Heat Island Amplitude:

$$\overline{\Delta A}_{x, Interpolated Warmest Month, Period_x} + \overline{A}_{x, Warmest Month, Modified} \quad (16)$$

Equation for Estimated Mean Warmest Month Air Temperature of the Urban Heat Island:

$$\overline{\Delta A}_{x, Interpolated Warmest Month, Period_x} + \overline{A}_{x, Warmest Month, Modified} + \overline{T}_{x, Interpolated Warmest Month, Rural, Period_x} \quad (17)$$

Equation for Total Mean Maximum Warmest Month Urban Heat Island Amplitude:

$$\overline{\Delta A}_{x, Interpolated, Maximum_{Warmest\ Month, Period_x}} + \overline{A}_{x, Maximum_{Warmest\ Month, Modified}} = \overline{A}_{x, Maximum_{Warmest\ Month}} \quad (18)$$

Equation for Estimated Mean Maximum Warmest Month Air Temperature of the Urban Heat Island:

$$\overline{\Delta T}_{x, Interpolated, Maximum_{Warmest\ Month, Period_x}} + \overline{T}_{x, Maximum_{Warmest\ Month, Modified}} = \overline{T}_{x, Maximum_{Warmest\ Month, Urban}} + \overline{T}_{x, Maximum, Interpolated_{Warmest\ Month, Rural, Period_x}} \quad (19)$$

In Equations (16)–(19), variables and subscripts are as in Equations (8)–(15). It should, however, be noted that:  $\overline{\Delta A}_{x, Interpolated_{Warmest\ Month, Period_x}}$  is as calculated in Equation (14);  $\overline{A}_{x, Warmest\ Month, Modified}$  is as calculated in Equation (5);  $\overline{T}_{x, Interpolated_{Warmest\ Month, Rural, Period_x}}$  is as calculated in Equations (8)–(10);  $\overline{\Delta A}_{x, Interpolated, Maximum_{Warmest\ Month, Period_x}}$  is as calculated in Equation (15);  $\overline{A}_{x, Maximum_{Warmest\ Month, Modified}}$  is as calculated in Equation (6); and  $\overline{T}_{x, Maximum, Interpolated_{Warmest\ Month, Rural, Period_x}}$  is as calculated in Equations (11)–(13).

In addition to the above, please note that Equations (16)–(19) may be used to calculate estimates of urban heat island amplitude and air temperature for a scenario that assumes no mitigation of the urban heat island effect. To do so, null values for the variables  $\Delta \bar{I}$ ,  $\Delta \bar{V}$ , and  $\Delta \bar{\alpha}$  in Equations (5) and (6), which feed into Equations (16)–(19) with the inclusion of the variables  $\overline{A}_{x, Warmest\ Month, Modified}$  and  $\overline{A}_{x, Maximum_{Warmest\ Month, Modified}}$  in same, are required.

### 2.2.3. Population Dynamics

Population dynamics are represented in the previously described cohort-component population projection. The first step in the cohort-component population projection is to compute the age cohort-specific fertility and mortality rates that are represented by the total numbers of births and deaths by age cohort between the past two official censuses, and then annualizing said rates. For instance, the age cohort-specific fertility rate is determined by calculating the total number of births that occurred to the population in a given age cohort during the period between the past two censuses and dividing said total by the size of the age cohort at the time of the last census; the quotient resulting from this operation is then divided by the number of years between the past two censuses in order to annualize the rate. The computation of the age cohort-specific mortality rate is performed in the same manner. Equations (20) and (21) demonstrate the computation of the age cohort-specific fertility and mortality rates, respectively.

Equation for Age Cohort-Specific Fertility Rate:

$$F_{Cohort\ x} = \frac{\left( \frac{\sum_{i=B_0}^{B_0-1} i_{Cohort\ x}}{P_0, Cohort\ x} \right)}{C_0 - C_{0-1}} \quad (20)$$

As related to Equation (20),  $F$  means age cohort-specific fertility rate,  $B$  means births in the respective cohort,  $P$  means population in the respective cohort, and  $C$  means year of census. Subscript notation relates to years of official censuses or the identification of a particular age cohort. To illustrate,  $C_0$  denotes the year of the immediate past census, whereas  $C_{0-1}$  denotes the year of the penultimate census. Similarly,  $P_0, Cohort\ x$  denotes population at the time of the last official census in a given age cohort. Please note that this equation is applied to all age cohorts.

Equation for Age Cohort-Specific Mortality Rate:

$$M_{Cohort\ x} = \frac{\left( \frac{\sum_{i=D_0}^{D_0-1} i_{Cohort\ x}}{P_{0, Cohort\ x}} \right)}{C_0 - C_{0-1}} \quad (21)$$

As related to Equation (21),  $M$  means age cohort-specific mortality rate and  $D$  means deaths. The meaning of all other notation in Equation (21) corresponds with that of Equation (20). Please note that this equation is applied to all age cohorts.

The part of population growth or decline that occurs between two points and is not attributable to births or deaths is attributable to net migration. Within the *UHIMPT* model, net migration is computed as the change in the population of a given age cohort between the past two censuses, minus the difference between the total number of births and deaths that are attributable to the population in the same age cohort between the past two official censuses, and then divided by the population of the age cohort at the time of the last census; the resulting quotient is then divided by the number of years between the past two censuses in order to annualize the rate. This is demonstrated in Equation (22).

Equation for Age Cohort-Specific Net Migration Rate:

$$N_{Cohort\ x} = \frac{\left( \frac{(P_{0, Cohort\ x} - P_{0-1, Cohort\ x}) - \left( \sum_{i=B_0}^{B_0-1} i_{Cohort\ x} - \sum_{i=D_0}^{D_0-1} i_{Cohort\ x} \right)}{P_{0, Cohort\ x}} \right)}{C_0 - C_{0-1}} \quad (22)$$

As related to Equation (22),  $N$  means age cohort-specific net migration rate. The meaning of all other notation in Equation (22) corresponds with that of Equations (20) and (21). Please note that this equation is applied to all age cohorts and may result in a positive or negative rate. Positive and negative rates indicate in-migration and out-migration, respectively.

With the annualized, age cohort-specific fertility, mortality and net migration rates having been calculated, future population can be projected. As is demonstrated in the following discussion, the projection methodology for the first and last age cohorts differs from that of all other age cohorts.

The first step in projecting population in the first age cohort is to compute the total number of births that can be expected to occur in all age cohorts during the current time step. This is done by applying the appropriate age cohort-specific fertility rate to the corresponding age cohort's population in the current time step, and then summing the result for all age cohorts to yield the total number of births that can be expected to occur throughout all age cohorts. Next, the impacts of mortality are accounted for by multiplying the total number of births that can be expected to occur in all age cohorts by the difference between one and the first age cohort's mortality rate. This results in an estimate of new population (i.e., births) that can be expected to survive to the next age cohort. Finally, the impacts of migration are accounted for by multiplying the first age cohort's net migration rate with the estimate of new population that can be expected to survive to the next age cohort, and then adding the product of this operation to said estimate in order to obtain the projection of future population in the first age cohort in the next time step. This is summarized in Equation (23).

Equation for Projection of Population in the First Age Cohort:

$$P_{x, Cohort\ 1} = \left( (1 - M_{Cohort\ 1}) \times \sum_{i=Cohort\ 1}^{Last\ Cohort} (F_i \times P_{x-1,i}) \right) + \left( (1 - M_{Cohort\ 1}) \times \sum_{i=Cohort\ 1}^{Last\ Cohort} (F_i \times P_{x-1,i}) \times N_{Cohort\ 1} \right). \quad (23)$$

In Equation (23), notation is as defined in, or follows the conventions of, Equations (20)–(22). It should, however, be noted that the subscript in  $P_{x, Cohort 1}$  denotes the population of the first age cohort in a given time step. Please note that this equation is only used to project the population of the first age cohort.

The first step in projecting population in the second through the penultimate age cohorts is to estimate the portion of the population of the preceding age cohort (i.e., the first through the antepenultimate age cohorts, as appropriate) in the current time step that can be expected to survive into the next age cohort. This is done by multiplying the population of the preceding age cohort in the current time step by the difference between one and its (i.e., the preceding age cohort's) mortality rate. The product that results from this operation serves as an estimate of the portion of the population of the preceding age cohort in the current time step that can be expected to survive into the next age cohort. Next, said estimate is multiplied with the respective age cohort-specific net migration rate in order to estimate the impacts of migration on the population size; the net migration rates of the preceding age cohort are used in this step. The impact of migration is then added to the aforesaid estimate in order to obtain the projected population of the respective age cohort in the next time step. This is summarized in Equation (24).

Equation for Projection of Population in the Second through the Penultimate Age Cohorts:

$$P_{x, Cohort x} = ((1 - M_{Cohort x-1}) \times P_{x-1, Cohort x-1}) + ((1 - M_{Cohort x-1}) \times P_{x-1, Cohort x-1} \times N_{Cohort x-1}). \quad (24)$$

The notation of Equation (24) is the same as, or follows the conventions of, Equations (20)–(23). It is, however, noted that the subscript in  $M_{Cohort x-1}$  signifies the preceding age cohort's mortality rate. Similarly, the subscript in  $P_{x, Cohort x-1}$  denotes the population of the preceding age cohort in a given time step. Please note that this equation is applied to all age cohorts except the first and last age cohorts.

To project the population of the last age cohort in the next time step, the portions of the populations of the penultimate and last age cohorts in the current time step that can be expected to survive into the next age cohort are computed by multiplying said populations with the difference between one and their respective mortality rates. The results of these operations are then summed to yield a total estimate of population in the penultimate and last age cohorts in the current time step that can be expected to survive into the next time step. Next, this estimate is multiplied with the net migration rate of the last age cohort in order to determine the impact of migration thereon. The impact of migration is then added to the aforesaid estimate in order to yield the projected population of the last age cohort in the next time step.

Equation for Projection of Population in the Last Age Cohort:

$$P_{x, Last Cohort} = ((1 - M_{Last Cohort}) \times P_{x-1, Last Cohort}) + ((1 - M_{Last Cohort-1}) \times P_{x-1, Last Cohort-1}) + \left( ((1 - M_{Last Cohort}) \times P_{x-1, Last Cohort} \times N_{Last Cohort}) + ((1 - M_{Last Cohort-1}) \times P_{x-1, Last Cohort-1} \times N_{Last Cohort-1}) \right). \quad (25)$$

The notation of Equation (25) follows the style and conventions of Equations (20)–(24). Please note that this equation is used to project the population of only the last age cohort.

The sum of the projected populations of all age cohorts in a given time step represents the total projected population in the UHIMPT model in the same time step.

Please note that the methodologies and operations that are detailed in this section draw primarily from Klosterman [46] and Smith et al. [47].

#### 2.2.4. Heat-Related Mortality

As has been discussed in Section 2.1, the UHIMPT model uses temperature–mortality functions of Nordio et al. [50]. These functions, which indicate the relative risk of mortality

according to normal mean summer and winter air temperatures in a given area, are programmed into the UHIMPT model and represented in Equations (26)–(33) (Note 19). Table 1, which follows Equations (26)–(33), provides an overview of the corresponding mean summer and winter air temperatures that correspond with each of the functions.

**Table 1.** Temperature–Mortality Functions by Corresponding Mean Summer and Winter Air Temperature.

Temperature–Mortality Function	Summer Air Temperature		Winter Air Temperature	
	Mean (°C)	Standard Deviation (SD)	Mean (°C)	Standard Deviation (SD)
Temperature–Mortality Function 1 ( $TM_1$ )	22.79	3.78	0.78	5.42
Temperature–Mortality Function 2 ( $TM_2$ )	21.31	3.81	−3.19	6.57
Temperature–Mortality Function 3 ( $TM_3$ )	23.90	3.54	0.40	6.58
Temperature–Mortality Function 4 ( $TM_4$ )	25.90	2.85	6.53	5.82
Temperature–Mortality Function 5 ( $TM_5$ )	19.67	3.79	9.54	4.57
Temperature–Mortality Function 6 ( $TM_6$ )	27.35	1.92	12.03	5.40
Temperature–Mortality Function 7 ( $TM_7$ )	27.74	1.57	17.59	4.87
Temperature–Mortality Function 8 ( $TM_8$ )	29.17	4.29	10.18	3.98

Source: Adapted from Nordio et al. [50].

Equation for Temperature–Mortality Function 1 ( $TM_1$ ):

$$R_{TM_1} = (2 \times 10^{-10})T^6 - (8 \times 10^{-10})T^5 - (6 \times 10^{-8})T^4 + (8 \times 10^{-7})T^3 + (9 \times 10^{-5})T^2 + 0.0017T + 0.9502. \quad (26)$$

Equation for Temperature–Mortality Function 2 ( $TM_2$ ):

$$R_{TM_2} = (3 \times 10^{-11})T^6 + (3 \times 10^{-9})T^5 + (7 \times 10^{-8})T^4 - (2 \times 10^{-7})T^3 + (5 \times 10^{-5})T^2 + 0.0013T + 0.9587. \quad (27)$$

Equation for Temperature–Mortality Function 3 ( $TM_3$ ):

$$R_{TM_3} = (2 \times 10^{-11})T^6 + (2 \times 10^{-9})T^5 + (3 \times 10^{-9})T^4 - (1 \times 10^{-6})T^3 + (1 \times 10^{-4})T^2 + 0.0011T + 0.9581. \quad (28)$$

Equation for Temperature–Mortality Function 4 ( $TM_4$ ):

$$R_{TM_4} = (1 \times 10^{-10})T^6 - (9 \times 10^{-10})T^5 - (1 \times 10^{-7})T^4 - (4 \times 10^{-7})T^3 + 0.0002T^2 - 0.0007T + 0.9753. \quad (29)$$

Equation for Temperature–Mortality Function 5 ( $TM_5$ ):

$$R_{TM_5} = (-8 \times 10^{-11})T^6 - (2 \times 10^{-9})T^5 + (5 \times 10^{-7})T^4 - (6 \times 10^{-6})T^3 + (6 \times 10^{-5})T^2 + 0.0019T + 0.9504. \quad (30)$$

Equation for Temperature–Mortality Function 6 ( $TM_6$ ):

$$R_{TM_6} = (3 \times 10^{-10})T^6 - (2 \times 10^{-8})T^5 + (1 \times 10^{-7})T^4 + (2 \times 10^{-6})T^3 + 0.0002T^2 - 0.0039T + 1.0121. \quad (31)$$

Equation for Temperature–Mortality Function 7 ( $TM_7$ ):

$$R_{TM_7} = (-6 \times 10^{-10})T^6 + (5 \times 10^{-8})T^5 - (1 \times 10^{-6})T^4 + (2 \times 10^{-5})T^3 + 0.0001T^2 - 0.0044T + 1.0179. \quad (32)$$

Equation for Temperature–Mortality Function 8 ( $TM_8$ ):

$$R_{TM_8} = (-4 \times 10^{-10})T^6 + (5 \times 10^{-8})T^5 - (2 \times 10^{-6})T^4 + (2 \times 10^{-5})T^3 + 0.0002T^2 - 0.0028T + 0.9741. \quad (33)$$

In Equations (26)–(33),  $R_{TM_x}$  represents relative risk of mortality as represented in a given temperature–mortality function (e.g., the relative risk of mortality in Temperature–Mortality Function 1 is represented as  $R_{TM_1}$ ), and  $T$  represents the air temperature of exposure in degrees Celsius (i.e., °C). Please note that the air temperature of exposure,  $T$ , as applied in the *UHIMPT* model, is  $\bar{T}_{x, \text{Warmest Month, Urban}}$ , which is calculated in Equation (17), or  $\bar{T}_{x, \text{Maximum Warmest Month, Urban}}$ , which is calculated in Equation (19).

As has been previously noted, the temperature–mortality functions of Nordio et al. [50], which are represented in Equations (26)–(33), correspond with mean summer and winter air temperatures in a given area. Table 1 provides an overview of the mean summer and winter air temperatures that correspond with each of the temperature–mortality functions.

Based on user-input data on normal mean summer and winter air temperatures for the region, the *UHIMPT* model selects the proper temperature–mortality function for application. This is done by: first computing the sum of the absolute differences between the user-input normal mean summer and winter air temperatures and those (i.e., the mean summer and winter air temperatures) that are representative of each of the temperature–mortality functions (see: Table 1); then, selecting the temperature–mortality function that results in the smallest absolute difference, as determined by the minimum of the entire set of sums of absolute differences. This is demonstrated in Equations (34) and (35).

Equation for Sum of Absolute Differences Between User-Input and Temperature–Mortality Function-Represented Mean Summer and Winter Air Temperatures:

$$D_{User, TM_x} = (|\bar{T}_{Summer, User} - \bar{T}_{Summer, TM_x}|) + (|\bar{T}_{Winter, User} - \bar{T}_{Winter, TM_x}|). \quad (34)$$

Equation for Selection of Temperature–Mortality Function with Smallest Sum of Absolute Differences Between User-Input and Temperature–Mortality Function-Represented Mean Summer and Winter Air Temperatures:

$$TM_{Applicable} = TM_x \text{ associated with } \min \left\{ \begin{array}{l} D_{User, TM_1}, D_{User, TM_2}, D_{User, TM_3}, D_{User, TM_4}, \\ D_{User, TM_5}, D_{User, TM_6}, D_{User, TM_7}, D_{User, TM_8} \end{array} \right\}. \quad (35)$$

In Equation (34),  $D_{User, TM_x}$  represents the sum of the absolute differences between user-input normal mean air temperatures and those reflected in a given temperature–mortality function,  $\bar{T}_{Summer, User}$  means the mean summer air temperature in degrees Celsius (i.e., °C) that is represented in the user-input data, and  $\bar{T}_{Winter, TM_x}$  means the mean winter air temperature in degrees Celsius that is represented by a given temperature–mortality function.

In Equation (35),  $TM_{Applicable}$  denotes the applicable temperature–mortality function. The variable  $TM_x$  denotes a given temperature–mortality function, which is defined as the temperature–mortality function that is associated with the minimum of the set of all sums of the absolute differences between user-input temperatures and those reflected in the eight temperature–mortality functions of Nordio et al. [50]; i.e.,  $D_{User, TM_1}$  through  $D_{User, TM_8}$ .

As has been previously stated, the *UHIMPT* model accounts for the human ability to acclimatize to higher temperatures. It does so by modifying the applicable temperature–mortality function with an acclimatization factor. This acclimatization factor is obtained

from the results of a meta-regression analysis by Nordio et al. [50], which indicates that every 5 °C increase in mean air temperature results in a 1.78 percent reduction in heat-related mortality (95-Percent CI: 0.82, 2.74). The UHIMPT model uses this reduction in heat-related mortality, but applies it continuously, such that every fractional degree increase in projected mean air temperature results in a corresponding percent reduction in heat-related mortality. This is done in order to represent acclimatization as a gradual and continuous process (see: [50,55]). This is summarized in Equation (36).

Equation for Determination of Acclimatization Factor:

$$A = \left( \frac{\left( \frac{1.78}{100} \right)}{5} \right) \times (\bar{T}_{S_x} - \bar{T}_{S_{x-1}}). \quad (36)$$

In Equation (36),  $A$  represents acclimatization factor. The variable  $\bar{T}$  represents mean annual air temperature for the region and its accompanying subscripts represent time steps, such that  $\bar{T}_{S_{x-1}}$  represents the previous time step and  $\bar{T}_{S_x}$  represents the current time step.

The result of Equation (36),  $A$ , is then multiplied by the applicable factor of relative risk of mortality, which is determined by the temperature–mortality function that is selected by Equation (35), and then subtracted from same. This results in the modification of the relative risk factor according to changes in mean air temperature (Note 20). Equation (37) demonstrates the application of the acclimatization factor against the relative risk factor.

Equation for Application of Acclimatization Factor to Relative Risk Factor:

$$R_{TM_{Applicable, Acclimatized}} = R_{TM_{Applicable}} - (A \times R_{TM_{Applicable}}). \quad (37)$$

In Equation (37):  $R_{TM_{Applicable}}$  represents the relative risk of mortality that is associated with the applicable temperature–mortality function, which is selected with Equation (35) and represented in one of Equations (26)–(33); and  $R_{TM_{Applicable, Acclimatized}}$  represents the relative risk of mortality that is associated with the applicable temperature–mortality function, as impacted by acclimatization. The variable  $A$  represents the acclimatization factor, which is calculated in Equation (36).

After having applied the acclimatization change factor to the relative risk of mortality, the total impact of heat-related mortality, and specifically the number of excess deaths that can be expected to result from one day of exposure to heat in the urban area, is estimated. This is done by: first applying the relative risk of mortality that is associated with the applicable temperature–mortality function and impacted by acclimatization, which is defined as  $R_{TM_{x, Acclimatized}}$  in Equation (37), to the mortality rate and population of each age cohort that is reflected in the UHIMPT model’s cohort-component population projection, and summing the results thereof; then subtracting the product of the mortality rate and population of each age cohort that is reflected in the UHIMPT model’s cohort-component population projection, and summing the results thereof; and finally dividing the difference by 365 (i.e., the total number of days in one year). The result of these operations is the total estimated number of excess deaths resulting from one day of exposure to heat in the urban area. This is demonstrated in Equation (38).

Equation for Total Estimated Increase in Mortality Resulting from One Day of Exposure to Heat in the Urban Area:

$$\Delta D_{Heat} = \left( \frac{\left( \sum_{i=Cohort\ 1}^{Last\ Cohort} \left( \left( R_{TM_{Applicable, Acclimatized}} \times M_{Cohort\ x} \right) \times P_{x, Cohort\ x} \right) \right) - \left( \sum_{i=Cohort\ 1}^{Last\ Cohort} \left( M_{Cohort\ x} \times P_{x, Cohort\ x} \right) \right)}{365} \right). \quad (38)$$

In Equation (38):  $\Delta D_{Heat}$  represents the total estimated excess deaths resulting from one day of exposure to heat in the urban area;  $R_{TM_{Applicable, Acclimatized}}$  is the relative risk of mortality that is associated with the applicable temperature–mortality function, as impacted by acclimatization and calculated in Equation (37);  $M_{Cohort\ x}$  represents age

cohort-specific mortality rate as calculated in Equation (21); and  $P_{x, Cohort\ x}$  represents the population of a given age cohort in a given time step, which is calculated by Equations (23)–(25).

Please note that Equation (38) is used to estimate excess deaths resulting from one day of exposure to heat, as represented by the projected mean warmest month and mean maximum warmest month temperatures. This is effectuated through its inclusion of the variable  $R_{TM, Applicable, Acclimatized}$ , which, as may be seen in Equations (34), (35) and (37), is ultimately derived from the temperature–mortality functions that are presented in Equations (26)–(33). As has been previously explained in this section, these temperature–mortality functions are used to obtain the relative risk of mortality that is associated with the projected mean warmest month and mean maximum warmest month temperatures.

### 3. Results

The foregoing equations and structures complete the foundation of the *UHIMPT* model. This section demonstrates how it may be applied in a given location in order to facilitate an improved understanding of the public health threat of heat within the urban heat island and, therewith, the informed development of policy for its mitigation.

#### 3.1. Illustrative Model Demonstration

The following illustrative model demonstration is made within the context of Philadelphia, Pennsylvania. Philadelphia was selected for the purposes of this demonstration as a result of the author’s familiarity with the area, as well as the fact that the Philadelphia region has a temperate climate with a normal mean annual air temperature that closely approximates that of the continental United States (n.b., data obtained from Wang et al. [56] indicate that the normal mean annual air temperature from 1981 through 2010 was 11.91 °C in the continental United States and just 0.34 °C higher [12.25 °C] in the Philadelphia–Camden–Wilmington, PA–NJ–DE–MD Metropolitan Statistical Area, which comprises Philadelphia and the surrounding region). It is noted, however, that the *UHIMPT* model may be applied in any study area (e.g., regional level, municipal level, sub-municipal level) for which sufficient data may be obtained. Philadelphia is only used as an illustrative example of *UHIMPT* model application for the purposes of this article.

The illustrative model demonstration is presented in three parts, as follows: preparation of the customized multiple linear regression model that is adapted for use in Equations (5) and (6); outline of data inputs the *UHIMPT* model; and simulation of hypothetical interventions.

##### 3.1.1. Preparation of Customized Multiple Linear Regression Model

The *UHIMPT* model requires the preparation of a multiple linear regression model wherein: the land surface temperature of the intended study area is the dependent variable; and the mean surface albedo and the mean proportions of impervious surface cover and vegetation in the intended study area are the independent variables. Said multiple linear regression model is developed with user-input data and adapted for inclusion in Equations (5) and (6). Specifically, the standard (i.e., beta [ $\beta$ ]) coefficients of the multiple linear regression model’s independent variables are incorporated into Equations (5) and (6), which have been introduced in Section 2.2, and are reproduced below with graphical annotations as Equations (5<sub>R</sub>) and (6<sub>R</sub>), respectively.

Equation for Modification of Mean Warmest Month Urban Heat Island Amplitude (Reproduced with Graphical Annotations):

$$\bar{A}_{x_{Warmest\ Month, Modified}} = \bar{A}_{x_{Warmest\ Month}} + \left( \left( \frac{\left( \left[ \beta_i \right] \times \Delta \bar{I} \right) - \left( \left[ \beta_v \right] \times \Delta \bar{V} \right) - \left( \left[ \beta_\alpha \right] \times \Delta \bar{\alpha} \right) - 2.82}{1.15} \right) + 2.452 \right). \quad (5_R)$$

Equation for Modification of Mean Maximum Warmest Month Urban Heat Island Amplitude (Reproduced with Graphical Annotations):

$$\bar{A}_{x, \text{Maximum Warmest Month, Modified}} = \bar{A}_{x, \text{Maximum Warmest Month}} + \left( \left( \frac{\left( \boxed{\beta_i} \times \Delta \bar{I} \right) - \left( \boxed{\beta_v} \times \Delta \bar{V} \right) - \left( \boxed{\beta_\alpha} \times \Delta \bar{\alpha} \right) - 2.82}{1.15} \right) + 2.452 \right). \quad (6_R)$$

In Equations (5<sub>R</sub>) and (6<sub>R</sub>), the standard (i.e., beta [ $\beta$ ]) coefficients of the multiple linear regression model's independent variables are boxed. The coefficient  $\beta_i$  represents the standard (i.e., beta [ $\beta$ ]) coefficient for mean proportion of impervious surface cover that results when the mean surface albedo and mean proportions of impervious surface cover and vegetation of a given area are regressed on its land surface temperature. The coefficient  $\beta_v$  represents the standard (i.e., beta [ $\beta$ ]) coefficient for mean proportion of vegetation that results when the mean surface albedo and mean proportions of impervious surface cover and vegetation of a given area are regressed on its land surface temperature, and, similarly, the coefficient  $\beta_\alpha$  represents the standard (i.e., beta [ $\beta$ ]) coefficient for mean surface albedo that results when the mean surface albedo and mean proportions of impervious surface cover and vegetation of a given area are regressed on its land surface temperature. Please refer to Section 2.2 for definitions of all other variables in Equations (5) and (6) as reproduced above as Equations (5<sub>R</sub>) and (6<sub>R</sub>).

The preparation of a multiple regression model is required to assign appropriate, study area-specific values to  $\beta_i$ ,  $\beta_v$  and  $\beta_\alpha$ . Data for the multiple regression model are derived from cloud-free, daytime satellite imagery or processed from available digital geographic data. Specifically, data on land surface temperature, as well as surface albedo and the proportion of vegetation, are derived from moderate-to high-resolution daytime satellite imagery (e.g., Landsat 8), and the proportion of impervious surface cover is derived and processed from locally or regionally available digital geographic data in shapefile format (n.b., in this example, impervious surface cover has been derived and processed from geospatial dataset published by the City of Philadelphia [see Supplement B]). Data points (i.e., records) for inclusion in the multiple linear regression model represent and are calculated from pixels in the satellite imagery, or, in the case of the proportion of impervious surface cover, are processed with a geographic information system software package (e.g., ArcGIS Desktop by ESRI, Inc. of Redlands, CA, USA) to represent conditions in geographical areas that are identical to those represented by pixels in the satellite imagery. The specifics of data derivation and processing (incl., land surface temperature, mean surface albedo, and the mean proportions of impervious surface cover and vegetation) are fully described in Supplement B.

For the purposes of this illustrative model demonstration, a multiple linear regression model that represents conditions in Philadelphia, Pennsylvania has been prepared with IBM SPSS Statistics (Release 25), which is a statistical analysis software package by IBM Corporation of Armonk, NY, USA. Data entered into the multiple linear regression model include the surface albedo, proportion of vegetation, proportion of impervious surface cover, and land surface temperature of every 30-m by 30-m area within Philadelphia, which was totally on land surface (Note 21); this dataset included a total of 379,419 records and was approximately normally distributed (see: Supplement B). The resulting multiple linear regression model indicated that when the impact on land surface temperature is predicted, surface albedo ( $N = 379,419$ ;  $\beta = -5.874$ ;  $p < 0.0005$ ; 95-Percent CI =  $-6.042, -5.707$ ), impervious surface cover ( $N = 379,419$ ;  $\beta = 2.103$ ;  $p < 0.0005$ ; 95-Percent CI =  $2.078, 2.128$ ), and the proportion of vegetation ( $N = 379,419$ ;  $\beta = -8.730$ ;  $p < 0.0005$ ; 95-Percent CI =  $-8.779, -8.681$ ) are highly significant predictors. The coefficient of multiple determination ( $r^2$ ) of the resulting multiple linear regression model is 0.63. Supplement B provides additional details on the preparation of the multiple linear regression model that is used in this illustrative model demonstration.

With the multiple linear regression model having been developed, its standard (i.e., beta [ $\beta$ ]) coefficients are entered into Equations (5) and (6), which are again reproduced below as Equations (5<sub>R</sub>) and (6<sub>R</sub>), respectively.

Equation for Modification of Mean Warmest Month Urban Heat Island Amplitude (Reproduced with Standard Coefficients of Illustrative Model Demonstration):

$$\bar{A}_{x, \text{Warmest Month, Modified}} = \bar{A}_{x, \text{Warmest Month}} + \left( \left( \frac{(2.103 \times \Delta \bar{I}) - (8.730 \times \Delta \bar{V}) - (5.874 \times \Delta \bar{\alpha}) - 2.82}{1.15} \right) + 2.452 \right). \quad (5_R)$$

Equation for Modification of Mean Maximum Warmest Month Urban Heat Island Amplitude (Reproduced with Standard Coefficients of Illustrative Model Demonstration):

$$\bar{A}_{x, \text{Maximum Warmest Month, Modified}} = \bar{A}_{x, \text{Maximum Warmest Month}} + \left( \left( \frac{(2.103 \times \Delta \bar{I}) - (8.730 \times \Delta \bar{V}) - (5.874 \times \Delta \bar{\alpha}) - 2.82}{1.15} \right) + 2.452 \right). \quad (6_R)$$

Equations (5) and (6), as reproduced above as Equations (5<sub>R</sub>) and (6<sub>R</sub>), are used to depict modification of the mean and mean maximum warmest month urban heat island amplitude in the illustrative demonstration of the *UHIMPT* model.

### 3.1.2. Outline of Data Inputs Used in Illustrative Model Demonstration

The data input requirements of the *UHIMPT* model have been outlined in Section 2.1. As shown therein, these input requirements are largely centered around: population counts by age cohort at the time of the penultimate and last censuses; information on the births and deaths that occurred between the penultimate and last censuses; projections of mean and mean maximum warmest month temperatures in the urban and rural areas; and projections of mean annual temperature in the region. The Philadelphia-specific data used in this illustrative demonstration of the *UHIMPT* model are provided in Supplement C. Please note that this data is in addition to the standard (i.e., beta [ $\beta$ ]) coefficients that have been discussed in Section 3.1.1.

### 3.1.3. Simulation of Hypothetical Intervention Scenarios

The *UHIMPT* model was run several times with the Philadelphia-specific standard (i.e., beta [ $\beta$ ]) coefficients in Equations (5) and (6), as well as other data-inputs, which have been described in Sections 3.1.1 and 3.1.2, respectively (n.b., a copy of the *UHIMPT* model with these data inputs is provided in STELLA file format in Supplement D). In each of the model runs, the values representing changes to mean surface albedo and the mean proportions of impervious surface cover and vegetation (i.e.,  $\Delta \bar{\alpha}$ ,  $\Delta \bar{I}$  and  $\Delta \bar{V}$  in Equations (5) and (6)) were modified to result in the following four hypothetical intervention scenarios for simulation:

- Increasing mean surface albedo, but making no changes to the mean proportions of vegetation or impervious surface cover;
- Increasing the mean proportion of vegetation, but making no changes to mean surface albedo or the mean proportion of impervious surface cover;
- Decreasing the mean proportion of impervious surface cover, but making no changes to mean surface albedo or the mean proportion of vegetation;
- Increasing mean surface albedo and the mean proportion of vegetation in equal amounts, while decreasing the mean proportion of impervious surface cover in an amount that is equal to the additive inverse of said increases.

The purpose of these four scenarios is to demonstrate the utility of the *UHIMPT* model in exploring: the issue of the urban heat island effect; and by estimating the minimum changes to mean surface albedo and the mean proportions of vegetation and impervious surface cover that would be needed in order to eliminate urban-rural temperature differences, the efficacy of hypothetical urban heat island mitigation measures.

### Increasing the Mean Surface Albedo

The illustrative model demonstration indicates that, when the proportion of mean surface albedo is increased, but no changes are made to the mean proportions of vegetation or impervious surface cover, an increase of between 0.0711 and 0.0748 would be sufficient to result in the elimination of a mean maximum warmest month urban–rural temperature difference from 2018 through 2100, with the required increase growing over time. On the other hand, to eliminate the mean warmest month urban–rural temperature difference from 2018 through 2100, an increase in mean surface albedo of between 0.2970 and 0.3099 would be required over the same period also with the required increase growing over time. The reason why a larger increase in mean surface average albedo would be required to eliminate the mean warmest month urban–rural temperature difference is that the normal mean warmest month urban–rural temperature difference is slightly more than four times larger than the mean maximum warmest month urban–rural temperature difference.

The impacts of increasing mean surface albedo on mortality are discussed at the end of this section.

### Increasing the Mean Proportion of Vegetation

The illustrative model demonstration indicates that, when the mean proportion of vegetation is increased, but no changes are made to mean surface albedo or the mean proportion of impervious surface cover, an increase of between 0.0480 and 0.0505 would be sufficient to result in the elimination of a mean maximum warmest month urban–rural temperature difference from 2018 through 2100, with the required increase growing over time. To eliminate the mean warmest month urban–rural temperature difference from 2018 through 2100, however, an increase in the mean proportion of vegetation of between 0.2002 and 0.2090 would be needed, also with the required increase growing over time. As was the case with mean surface albedo, the fact that the normal mean warmest month urban–rural temperature difference is slightly more than four times larger than that of the mean maximum warmest month temperature results in the need for a larger increase in the mean proportion of vegetation to eliminate the mean warmest month urban–rural temperature difference than would be required to eliminate the mean maximum warmest month urban–rural temperature difference.

The impacts of increasing the mean proportion of vegetation on mortality are discussed at the end of this section.

### Decreasing the Mean Proportion of Impervious Surface

The illustrative model demonstration indicates that, when the mean proportion of impervious surface cover is decreased, but no changes are made to mean surface albedo or the mean proportion of vegetation, a decrease of between 0.2097 and 0.2206 would be sufficient to result in the elimination of a mean maximum warmest month urban–rural temperature difference from 2018 through 2100, with the required decrease growing over time. To eliminate the mean warmest month urban–rural temperature difference from 2018 through 2100, however, a decrease in the mean proportion of impervious surface cover of between 0.8759 and 0.9142 would be needed, also with the required decrease growing over time. As was the case with mean surface albedo and the mean proportion of vegetation, the need for a larger decrease in the mean proportion of impervious surface cover to eliminate the mean warmest month urban–rural temperature difference than would be required to eliminate the mean maximum warmest month urban–rural temperature difference is explained by the fact that the normal mean warmest month urban–rural temperature difference is slightly more than four times larger than that of the mean maximum warmest month temperature.

The impacts of decreasing the mean proportion of impervious surface cover on mortality are discussed at the end of this section.

### Simultaneously Increasing Mean Surface Albedo and the Mean Proportion of Vegetation, and Decreasing the Mean Proportion of Impervious Surface

The illustrative model demonstration indicates that, when mean surface albedo and the mean proportion of vegetation are increased in equal amounts, and the mean proportion of impervious surface cover is decreased in an amount that is equal to the additive inverse of the increases to mean surface albedo and the mean proportion of vegetation, the following changes would be sufficient to result in the elimination of a mean maximum warmest month urban–rural temperature difference from 2018 through 2100: an increase of between 0.0252 and 0.0265 in mean surface albedo and the mean proportion of vegetation, with the required increase growing over time; and a decrease of between 0.0252 and 0.0265 in the mean proportion of impervious surface cover, with the required decrease growing over time. Similarly, the following changes would be sufficient to result in the elimination of the mean warmest month urban–rural temperature difference from 2018 through 2100: an increase of between 0.1052 and 0.1098 in mean surface albedo and the mean proportion of vegetation, with the required increase growing over time; and a decrease of between 0.1052 and 0.1098 in the mean proportion of impervious surface cover, with the required decrease growing over time. As in all other scenarios, the fact that the normal mean warmest month urban–rural temperature difference is slightly more than four times larger than that of the mean maximum warmest month temperature results in a need for more significant changes to eliminate the mean warmest month urban–rural temperature difference than would be required to eliminate the mean maximum warmest month urban–rural temperature difference.

The mortality-related impacts of simultaneously increasing mean surface albedo and the mean proportion of vegetation, and decreasing the mean proportion of impervious surface cover, are discussed in the next subsection.

#### Mortality Impacts of all Hypothetical Scenarios

In each of the four aforementioned scenarios, between 41.65 and 144.66 deaths would result from one day of exposure to the mean maximum warmest month temperature if the respective interventions (*viz.*: increasing mean surface albedo; increasing the mean proportion of vegetation; decreasing the mean proportion of impervious surface cover; and the combination of increasing mean surface albedo, increasing the mean proportion of vegetation, and decreasing the mean proportion of impervious surface cover) were made, with the number of deaths increasing over the period from 2018 through 2100. This is between 0.40 and 1.49, or 0.95 and 1.02 percent, less than the number of deaths that would result from one day of exposure to the mean maximum warmest month temperature if no interventions to address the urban heat island effect by eliminating the mean maximum warmest month urban–rural temperature difference were taken.

With regard to the number of deaths that would result from one day of exposure to the mean warmest month temperature if the respective interventions were made, it is noted that, in each of the four scenarios, between 37.50 and 130.02 deaths would result, with the number of deaths growing over the period from 2018 through 2100. This is between 0.79 and 2.91, or 2.06 and 2.19 percent, less than the number of deaths that would result from one day of exposure to the mean warmest month temperature if no interventions to address the urban heat island effect by eliminating the mean warmest month urban–rural temperature difference were taken.

Please note that, in this illustrative demonstration, the impacts on mortality are the same among all four scenarios because their interventions are of the same magnitude. Indeed, each scenario's intervention has been designed to be sufficient to eliminate the urban–rural temperature difference.

In addition to the above, please note that acclimatization would have no substantial impact on heat-related mortality in each of the four aforementioned scenarios. Indeed, the total impact of acclimatization on the number of deaths resulting from one day of exposure to the mean and mean maximum warmest month temperatures with the simulated urban

heat island mitigation measures in place would be less than 0.001 deaths in 2100. Overall, from 2018 through 2100, the impact of acclimatization on the relative risk of heat-related mortality, based on the simulated conditions of this illustrative demonstration of the *UHIMPT* model, would only be slightly less than 1.23 percent. Thus, the gap between the commonly perceived threat of heat in urban areas, which generally does not account for acclimatization, and the actual threat, which accounts for acclimatization, is, based upon the simulated conditions, very small.

## 4. Discussion

### 4.1. Results of Illustrative Model Demonstration

As shown in Section 3, Philadelphia-specific inputs were used in the *UHIMPT* model for the purpose of conducting an illustrative demonstration of its utility. The final step in said demonstration was the simulation of hypothetical urban heat island intervention scenarios. These scenarios provide valuable insight, which can be used to inform the policy development. To illustrate, the three hypothetical scenarios wherein mean surface albedo and the mean proportions of vegetation and impervious surface cover are modified individually reveal that increasing the mean proportion of vegetation would require the smallest modification to eliminate urban–rural temperature differences. Thus, according to this illustrative demonstration of the *UHIMPT* model, increasing the mean proportion of vegetation would have the greatest impact in urban heat island mitigation. This may help to explain why, as is demonstrated in Dare [32], efforts to increase latent heat flux by increasing the abundance of vegetation and other measures are the current focal point of urban heat island mitigation policy. Naturally, the amenability and immediately visible co-benefits of increasing the mean proportion of vegetation (e.g., improved aesthetics; expanded open space area) may also help to explain their place at the current focal point of urban heat island mitigation policy [32].

In addition, it is noted that although the illustrative model demonstration shows that mean proportion of vegetation would require the smallest increase to eliminate urban–rural temperature differences, the amount of increase needed begs the question of whether or not effectuating such an increase is possible. Indeed, the illustrative demonstration of the *UHIMPT* model shows that to eliminate the mean warmest month urban–rural temperature difference through 2100, an increase of 0.2090 in the mean proportion of vegetation would be needed. Currently, the mean proportion of vegetation within Philadelphia is approximately 0.3762. Thus, if the mean proportion of vegetation were increased in a manner that is sufficient to eliminate the mean warmest month urban–rural temperature difference through 2100, the total mean proportion of vegetation within Philadelphia would need to be 0.5852. Clearly, attaining such a high mean proportion of vegetation would be extremely ambitious, if not impossible. As stated, however, the mean proportion of vegetation would require the smallest increase to eliminate urban–rural temperature differences. The mean proportion of impervious surface cover, on the other hand, would require the greatest change in order to eliminate the mean warmest month urban–rural temperature difference through 2100. When it is considered that a decrease of 0.9142 in the proportion of impervious surface cover would be required to eliminate the mean warmest month urban–rural temperature difference through 2100, and that the current mean proportion of impervious surface cover within Philadelphia is approximately 0.5540, the unlikelihood of attaining said decrease becomes abundantly clear.

Based on the above, the illustrative demonstration of the *UHIMPT* model makes it clear that eliminating urban–rural temperature differences by modifying just one of mean surface albedo, the mean proportion of vegetation, or the mean proportion of impervious surface cover, would be very difficult to impossible. If, however, efforts are made to simultaneously modify mean surface albedo, the mean proportion of vegetation, and the mean proportion of impervious surface cover, the goal of eliminating urban–rural temperature differences becomes much more attainable. Indeed, according to the illustrative demonstration, increases of 0.1098 in the mean surface albedo and the mean proportion of

vegetation, and a decrease of 0.1098 in the mean proportion of impervious surface cover, would be required if all three of these three variables were simultaneously modified in equal magnitudes. Obviously, these modifications would be much more readily effectuated than the modifications required to eliminate urban–rural temperature differences that are indicated by the three scenarios wherein mean surface albedo, the mean proportion of vegetation, and the mean proportion of impervious surface cover are modified individually and in isolation from one another. This suggests that it is important to address the issue of urban heat island mitigation with a multifaceted approach, rather than concentrating on one mitigation approach in particular.

Finally, and in addition to the above, it is noted that the fact that the illustrative demonstration of the *UHIMPT* model shows that only very small reductions in mortality would result from the simulated interventions demonstrates that land use planning and design can be only a part of the response to the issue of the urban heat island effect. Indeed, effectively and comprehensively addressing the risk of heat-related mortality in urban areas would require a coordinated and multifaceted response from a variety of perspectives. In particular, responses to the issue of heat-related mortality in urban areas from a public health and emergency management perspective would be critical in minimizing future risk.

#### 4.2. *UHIMPT* Model Potential

As shown in the illustrative demonstration that was presented in Section 3, the *UHIMPT* model provides a facilitated means of understanding the public health threat of heat within the urban heat island, as well as assessing the potential impacts of hypothetical urban heat island mitigation scenarios over an extended period. It does so by using modification of surface albedo and the proportions of vegetation and impervious surface cover as proxies for frequently prescribed approaches to urban heat island mitigation, and simulating the potential results of such modification, as impacted by future climate change and the human ability for acclimatization to higher air temperatures. The information it yields may be translated into policy for urban heat island mitigation (e.g., information resulting from hypothetical scenarios related to modification of surface albedo may be translated into cool roof requirements with specific performance standards).

Based on the foregoing, one may conclude that use of the *UHIMPT* model has the potential to increase the efficiency and precision of the policy development process as related to urban heat island mitigation. Indeed, it can support the development of reasoned and targeted urban heat island mitigation policy by facilitating the assessment of potential results of planned policy before implementation, thereby preventing the adoption of policy that is ineffective or may have undesired outcomes. Similarly, the *UHIMPT* model can help to improve the goal-setting process by providing insight into the extent of change that is needed to effectively mitigate the urban heat island, and the feasibility thereof. This promotes the definition and adoption of realistic and achievable goals that inspire action.

In addition to the above, it is noted that the *UHIMPT* model's customizability for application in any given area serves to ensure the accuracy of its outputs. This customizability promotes increased efficiency and precision of the policy development process by ensuring the validity of model outputs, and confidence therein. Moreover, the range of parameters in the *UHIMPT* model, which draw from a variety of published studies (e.g.,: temperature–mortality functions and acclimatization factor of Nordio et al. [50]; the population size–urban heat island amplitude function of Oke [34]; the land surface temperature–air temperature modeling of Gallo et al. [30]), provide urban planning and related professionals (i.e., intended users of the *UHIMPT* model) with access to relevant and useful information that may be from fields outside of their specific area of expertise. This further supports the policy development process not only with the information provided, but also by incorporating a plurality of perspectives in developing policy responses.

## 5. Model Validation

The *UHIMPT* model is intended to be used to estimate the potential impacts of hypothetical urban heat island mitigation strategies on heat-related mortality. Given its intended use, the critical aspects of model validation are: whether or not the model structure represents actual conditions accurately and in sufficient detail; and if simulated behavior reasonably mimics observed behavior to a degree that is sufficient to instill confidence in the model [57–59]. Both of these aspects of model validation are addressed in the following sections.

### 5.1. Structural Validation

To validate the structure of the *UHIMPT* model, the boundary adequacy, structure verification, and parameter verification tests of Forrester and Senge [57] have been applied.

#### 5.1.1. Boundary Adequacy

The purpose of the boundary adequacy test is to determine if the model includes the relevant concepts and structures that are necessary to fulfill its intended purpose [57,59], which, as previously stated, is to estimate the potential impacts of hypothetical urban heat island mitigation strategies on heat-related mortality. With this purpose having been stated, it is noted that the *UHIMPT* model includes the following structures and concepts:

- Urban heat island amplitude, as affected by population size, which is used as a proxy for development intensity, and the application of hypothetical urban heat island mitigation measures;
- Climate change impacts, and specifically the annualized projections of mean and mean maximum warmest month temperatures;
- A cohort–component population projection, which impacts urban heat island amplitude with its projection of total population and is also used in the estimation of future heat-related mortality;
- Future heat-related mortality, which is driven by: the mortality calculations of the cohort–component population projection, and temperature–mortality functions and an acclimatization factor, all of which have been developed by Nordio et al. [50].

Each of the aforementioned structures and concepts is endogenous to the *UHIMPT* model. They are, however, impacted by built-in functions from published studies, including: the population size–urban heat island amplitude function for North American settlements of Oke [34]; a linear regression model by Gallo et al. [30] wherein air temperature is the independent variable and land surface temperature is the dependent variable; and the temperature–mortality functions and acclimatization factor of Nordio et al. [50]. In addition, the aforementioned structures and concepts are impacted by a variety of user-input data, which has been discussed in Section 2.1.

The aforementioned concepts and structures are sufficient to fulfill the purpose of the *UHIMPT* model. Indeed, they enable the user to estimate the potential impacts of hypothetical urban heat island mitigation strategies on heat-related mortality, as impacted by population growth and development, climate change impacts on temperature, and acclimatization to higher temperatures. Nonetheless, it is acknowledged that use of the *UHIMPT* model for any other purpose may require adaptation of same, which may result in the need for boundary modification.

#### 5.1.2. Structure Verification

The structure verification test is focused on comparing the structure of the model with that of the actual system it represents [57]. This section applies the structure verification test to the *UHIMPT* model.

##### Structure of Actual System

With regard to the structure of the actual system, it is noted that the urban heat island effect is primarily the result of the impacts of the built environment on surface energy

balance [27]. Under development trajectories wherein no efforts to mitigate the urban heat island effect are made, a preponderance of low-albedo surfaces and areas with reduced latent heat flux are largely responsible for urban heat island formation [60]. The intensity of the urban heat island effect is generally coupled with the intensity of development in the built environment. Indeed, highly intense levels of physical development in the built environment generally result in increased urban heat island amplitude (see: [61]).

Exposure to high temperatures in the urban heat island increases the relative risk of mortality [26,27]. This increased relative risk of mortality is exacerbated by the fact that climate change is also expected to result in higher temperatures (see: [9]). Indeed, not only does the urban heat island effect result in higher temperatures in the urban area, but climate change may be expected to result in higher temperatures overall. However, research indicates that humans have a capacity to gradually acclimatize to higher temperatures (see: [50,55]). Thus, the increased relative risk of mortality is counterbalanced by the human capacity for acclimatization.

Mortality, however, does not maintain a constant rate among all age cohorts. Indeed, mortality rates vary among age cohorts, with the mortality rate for infants typically being higher than for young children and adolescents, and the mortality rate for post-adolescence age cohorts generally tending to increase with age [47]. This must be accounted for when simulating the impacts of heat exposure on future heat-related mortality.

#### Structure of UHIMPT Model

With regard to the structure of the *UHIMPT* model, it is noted that initial urban heat island amplitude is derived from the normal temperatures in the urban and rural (i.e., surrounding) areas. As urban development occurs, however, urban heat island amplitude increases. The *UHIMPT* model uses simulated population size as a proxy for urban development and means of determining future urban heat island amplitude in accordance with the population size–urban heat island amplitude function for North American settlements of Oke [34]. This function uses population size as a proxy for urban development intensity and, therewith, increased urban heat island amplitude (n.b., use of population size as a proxy for urban development intensity is explained by the fact that increased population creates a need for increased housing opportunities, commercial and retail space, and supporting infrastructure). Simulated population size, however, is not the only determinant of future urban heat island amplitude. Indeed, the *UHIMPT* model also provides a means of simulating modification of the urban heat island amplitude. It does so by providing the user a means of altering the mean surface albedo and the mean proportions of impervious surface and vegetation, both of which have an impact on latent heat flux.

In addition to the above, the *UHIMPT* model accounts for the impacts of climate change by incorporating user-input temperature projections for future periods in the urban and rural (i.e., surrounding) areas, and annualizing same projections over the course of the simulated period. This results in an accounting of the impacts of climate change on temperature, both generally and on urban heat island amplitude in particular. When the simulated urban heat island amplitude at a given time step, which, to clarify, may be defined as the urban–rural temperature difference, is added to the simulated temperature of the rural area at the same time step, the total simulated temperature in the urban area at the given time step results.

The total simulated temperature in the urban area impacts relative risk of mortality, which is determined in accordance with climate-specific temperature–mortality functions of Nordio et al. [50]. In the *UHIMPT* model, however, the relative risk of mortality is adjusted to account for acclimatization by means of the acclimatization factor of Nordio et al. [50]. This adjustment is made on the basis of change to the mean annual temperature of the region (i.e., the combination of urban and rural areas), and not just that of the urban area. This is based on the knowledge that human populations are, as a whole, not sedentary and travel on a frequent basis (e.g., when commuting to a place of employment).

Finally, the *UHIMPT* model uses the adjusted relative risk factors to simulate the impacts of exposure to heat within the urban heat island. It does so by multiplying the adjusted relative risk factor by the calculated daily mean number of deaths in each age cohort. The results of this operation for each age cohort are then summed to obtain a total number of deaths per day of exposure to heat in the urban heat island.

#### Result of Structure Verification Test

The generalities of the actual system and the *UHIMPT* model have been described in this section. Based on these descriptions, it is apparent that *UHIMPT* model does not contradict knowledge about the actual system it represents. Thus, the structure of the *UHIMPT* model is verified.

#### 5.1.3. Parameter Verification

With regard to parameterization, it is noted that several parts of the *UHIMPT* model use specialized information from published studies, which extend beyond the particular user-input data requirements that have been discussed in Section 2.1 and detailed in Supplement A. These include: an adaptation of the population size–urban heat island amplitude function for North American settlements of Oke [34], which is included in Equations (3) and (4); a linear regression model by Gallo et al. [30], which is incorporated into Equations (5) and (6) and provides a means of estimating air temperature from land surface temperature; the temperature–mortality functions of Nordio et al. [50], which are represented in Equations (26)–(33) and provide a means of computing relative risk of mortality according to local climate and temperature of exposure; and the acclimatization factor that results from a meta-regression analysis by Nordio et al. [50] and is incorporated into Equation (36). The validity of this specialized information is discussed, upon introduction, in Section 2.2; and fully detailed in Oke [34], Gallo et al. [30] and Nordio et al. [50], as applicable.

#### 5.2. Behavioral Validation

Behavioral validation is focused on whether or not the model's behavior reasonably mimics the observed behavior of the actual system [57]. When conducting the illustrative demonstration of the *UHIMPT* model that is presented in Section 3.1, efforts were made to proof the simulated behavior against the behavior that could be expected to occur in the actual system. This proofing of the *UHIMPT* model revealed no anomalies. The model behaved as one would expect of the actual system, with and without the application of hypothetical urban heat island mitigation measures.

## 6. Model Limitations

As with any model, there are limitations associated with the *UHIMPT* model. The following sections outline known limitations of the *UHIMPT* model.

#### 6.1. Total Impact of Multi-Day Extreme Events

A key limitation of the *UHIMPT* model is that it does not simulate the total impact of heat-related mortality over multi-day extreme heat events (i.e., heatwaves). Such events may result in uneven patterns of mortality resulting from the thermoregulatory capacities of various populations, the potential for behavioral modification caused by prolonged heat exposure, when the heatwave occurs, emergency response management, and a variety of other factors (see: [62–65]). The *UHIMPT* model, however, simulates the impacts of one day of same-day exposure to the mean warmest month and mean maximum warmest month temperature on mortality. It does not simulate the impacts over multi-day periods and should under no circumstances be used to derive estimates of same (e.g., by multiplying the simulated impacts of one day of same-day exposure to the mean warmest month and mean maximum warmest month temperature on mortality by the number of days in a hypothetical extreme heat event). Nonetheless, the risk of mortality resulting from exposure to heat is generally highest on the same day of exposure [50,62,66]. Thus, the

*UHIMPT* model's simulation of the impacts of one day of same-day exposure to the mean warmest month and mean maximum warmest month temperature on mortality helps to illustrate a worst-case scenario.

### 6.2. Accidental Mortality

The *UHIMPT* model does not account for accidental mortality. Accidental mortality, however, may be associated with behavioral modification caused by extreme heat events (see: [64,65,67]). For instance, high temperatures may cause various populations to seek relief by swimming, which may cause a spike in drownings. This is demonstrated by Basagaña et al. [64], who show that the relative risk of mortality from accidental drowning on extremely hot days may be greater than 2.0. Such deaths are not accounted for by the *UHIMPT* model because, vis-à-vis non-accidental mortality, there are few studies on the subject from which to draw.

### 6.3. Assumption of Constant Growth or Stagnant Conditions in the Built Environment

An additional limitation of the *UHIMPT* model is associated with its accounting of the dynamic nature of urban heat island amplitude, which uses population size as a proxy for development intensity and, therewith, urban heat island intensity, and assumes constant growth or stagnant conditions in the built environment. In the event of a decline in population, the *UHIMPT* model assumes no contraction of the built environment, which could be expected to result in decreased development intensity and an associated reduction in urban heat island intensity. Such contractions of the built environment have been observed in parts of the United States (e.g., Ohio, Pennsylvania) and eastern Germany (see: [68,69]), where, for instance, renaturation has been proposed as a means of addressing the phenomenon (i.e., population decline) and associated problems of disused properties (see: [70,71]). The *UHIMPT* model does not simulate such contractions of the built environment because it is assumed that any contraction would be associated with a significant and highly variable lag time that cannot be sufficiently modeled with a reasonable degree of accuracy. This limitation can, however, be overcome by providing updated data inputs and rerunning the model at any point in the future. By doing so, new baseline urban–rural temperature differences would be established, and inaccuracies minimized. Nonetheless, the *UHIMPT* model should not be employed in cases where there is a sustained decline in population.

### 6.4. Assumption of Constant Mortality, Fertility and Net Migration Rates

The *UHIMPT* model's cohort-component population projection assumes that mortality, fertility and net migration rates remain constant. As has been described in Section 2.1.1, however, this assumption is consistent with common practice (see: [46,47]) and reduces user-input data requirements. This assumption has also been made because, as noted in Smith et al. [47], there is a lack of scientific reasoning that proves that such rates can be accurately projected on the basis of historic information, particularly in small areas (e.g., a municipality), and past attempts to project such rates have not proven to be highly successful. In addition to the assumption of constant mortality, fertility and net migration rates, the *UHIMPT* model's population projection does not assume an upper limit to growth. Although a municipality's population growth potential would, ultimately, be limited by local development capacity, the *UHIMPT* model's population projection does not assume an upper limit to growth in order to reduce user-input data requirements (Note 22). To overcome these limitations, the user may provide updated data inputs for the population projection as described in Section 2.1.2 and rerun the model. By doing so, updated mortality, fertility and net migration rates would be obtained.

### 6.5. Unforeseen Circumstances

The *UHIMPT* model does not account for the potential for unforeseen political, economic, land use, administrative or regulatory changes or similar circumstances that may

impact urban heat island formation. To illustrate, some hypothetical examples of such changes are: recession and economic downturn; changes in land use cover that are unrelated to the *UHIMPT* model's ability to test the impacts of changes to mean surface albedo, mean proportion of vegetation, and mean proportion of impervious surface; changes to municipal boundaries resulting from municipal mergers, demergers and other administrative changes; and the introduction of regional development policy that results in the alteration of historic development rates. While it would be impossible to develop the *UHIMPT* model to account for every possible scenario that may impact urban heat island formation, many would likely impact population dynamics. Thus, the impact of unforeseen changes that are not accounted for in the *UHIMPT* model can be accounted for by providing updated data inputs and rerunning the model.

#### 6.6. Limitations of Population Size–Urban Heat Island Amplitude Function

Although the population size–urban heat island amplitude function of Oke [34] provides the most comprehensive analysis of the relationship between population size and urban heat island amplitude in North American cities available to date, and the methodology with which it was produced has proven to be highly reliable in several subsequent studies (see: [39–41]), it is aging. In the event that an updated population size–urban heat island amplitude function becomes available, the model, and specifically Equations (3) and (4) as detailed in Section 2.2.1, should be revised to include same (Note 23).

With further regard to the population size–urban heat island amplitude function of Oke [34], it is noted that said function represents nighttime urban heat island amplitude, which is generally greater than daytime urban heat island amplitude because rural areas tend to cool at a faster rate than urban areas. However, the *UHIMPT* model's baseline measurement of urban heat island amplitude is not derived from nighttime-specific data (n.b., as explained in Section 2.1.2 and Section 2.2.1, the *UHIMPT* model's baseline measurement of urban heat island amplitude is derived from: normal mean warmest month air temperature, which is influenced by daytime and nighttime temperature; and normal mean maximum warmest month air temperature, which, because highest temperatures tend to occur during the afternoon, is influenced by daytime temperature). As a result, the magnitude of increase in urban heat island amplitude may be overstated. Although there have been several studies on the significance of diurnal variation in urban heat island amplitude (see: [27]), none have been as comprehensive or proven to be as reliable over a broad geographic area as the study upon which Oke's [34] population size–urban heat island amplitude function was developed. Thus, in the absence of a population size–urban heat island amplitude function that represents mean or daytime urban heat island amplitude, the use of Oke's [34] population size–urban heat island amplitude function in the *UHIMPT* model is justified. Nonetheless, it is noted that this issue can be addressed by providing updated baseline climate information as it becomes available and subsequently rerunning the *UHIMPT* model. Additionally, the modularity of the system dynamics approach provides the opportunity to revise the *UHIMPT* model to incorporate a different population size–urban heat island amplitude function or include an appropriate adjustment at a later date.

#### 6.7. Conversion of Land Surface Temperature to Air Temperature

In order to convert the simulated impacts of alterations of surface albedo, impervious surface cover and the proportion of vegetation on land surface temperature to air temperature, the *UHIMPT* model incorporates an adaptation of the linear regression model of Gallo et al. [30]. Said linear regression model, which is based on a comparison of air temperature and land surface temperature data collected at 14 meteorological observation stations located throughout the continental United States, represents cloud-free, daytime conditions. As such, it can only be used to simulate cloud-free, daytime conditions; it cannot represent the range of other possible conditions (e.g., cloudy, nighttime). This, however, is consistent

with the UHIMPT model's use of satellite-derived data representing cloud-free, daytime conditions in the development of the customized multiple linear regression model that is incorporated into Equations (5) and (6) and discussed at several points in Sections 2 and 3, as well as in Supplement B.

In addition to the above, it is reiterated that the aforementioned linear regression model of Gallo et al. [30] is not location-specific, but rather based on data collected at 14 meteorological observation stations located throughout the continental United States. Although their model explains 88 percent of the variability in the collected data (i.e.,  $r^2 = 0.88$ ), local analysis of the relationship between land surface temperature and air temperature in a given study area may result in a more reliable model. In the event that a more reliable, location-specific model becomes available, revision of the UHIMPT model to incorporate same should be considered. Note that the modularity of the system dynamics approach affords the opportunity to easily make such revisions.

#### 6.8. Selection of Appropriate Temperature–Mortality Function

As noted in Section 2.1.1, the temperature–mortality functions of Nordio et al. [50] have been developed with the benefit of a cluster analysis, which identified eight climate clusters covering the continental United States based on relative humidity, mean summer and winter air temperatures, and the standard deviation of mean summer and winter air temperatures. For each of these climate clusters, Nordio et al. [50] prepared a corresponding temperature–mortality function; all of these temperature–mortality functions have been incorporated into the UHIMPT model.

Although relative humidity, mean summer and winter air temperatures, and the standard deviation of mean summer and winter air temperatures have been used to identify clusters and, therewith, define the sample from which temperature–mortality functions were prepared, the UHIMPT model, as demonstrated in Equations (34) and (35), identifies the most applicable temperature–mortality function for a given area on the basis of mean summer and winter air temperatures alone. By doing so, the UHIMPT model's data input requirements are minimized.

While identification of the most applicable temperature–mortality function for a given area with the addition of information on relative humidity and the standard deviation of mean summer and winter air temperatures may, in theory, improve the identification of the most applicable temperature–mortality function for a given area, incorporation of such information results in a significantly increased burden on the user to input data. Moreover, the UHIMPT model's approach to selection of the appropriate temperature–mortality function for a given area already results in a reasonable degree of accuracy. This has been confirmed by testing at the time of model parameterization, which revealed that the UHIMPT model approach was able to: select the temperature–mortality function for the same climate cluster as provided by Nordio et al. [50] in 35 of 48 cases; and select the temperature–mortality function for a climate cluster that was, as regarded from the standpoint of air temperature, closely similar to the climate cluster as provided by Nordio et al. [50] in eight of 48 cases (Note 24). Thus, the UHIMPT model approach results in a reasonable degree of accuracy with the temperature–mortality function for the same or closely similar climate cluster as provided in Nordio et al. [50] being selected in 43, or 89.6 percent, of 48 cases (Note 25).

### 7. Proper Model Use

Given the limitations that have been discussed in Section 6, it is important to consider the UHIMPT model's proper use. In this regard, it is noted that the UHIMPT model should not simply be run once and never revisited after its initial outputs have been obtained. Indeed, the UHIMPT model should be periodically rerun as updated data inputs become available. This is particularly important in the case of the UHIMPT model's population projection, which, as has been discussed in Section 6, assumes constant mortality, fertility and net migration rates in the projected period. By rerunning the model as updated data

inputs become available, the impacts of new phenomena and trends on the components of the *UHIMPT* model can be captured and, therewith, the accuracy of its outputs can be maximized.

In addition to the above, it is noted that, given the necessary simplification of the real-world phenomena that are represented in the *UHIMPT* model, its outputs should not be used as definitive, long-term projections of future urban heat island amplitude. Rather, it should only be used to facilitate the development of generalized estimates of the potential impacts of hypothetical urban heat island mitigation strategies on heat-related mortality. Using the *UHIMPT* model in this manner provides a means of obtaining valuable information to support the development of targeted policy for urban heat island mitigation.

## 8. Conclusions

The *UHIMPT* model represents a new approach to estimate the potential impacts of hypothetical urban heat island mitigation strategies on heat-related mortality. It provides a high degree of customizability and, as has been demonstrated within the context of Philadelphia, Pennsylvania, yields important information that can inform the policy development process.

## 9. Notes

1. Please note that although data on normal extreme maximum temperature exists (e.g., the dataset that is presented in Wang et al. [56] includes data for extreme maximum temperature over thirty years), the *UHIMPT* model uses normal mean maximum warmest month temperature in its accounting for the urban heat island effect. Both indicators represent extremes with: normal mean maximum warmest month temperature able to be considered as the mean extreme; and the normal extreme maximum temperature able to be considered as the extreme of extremes. The *UHIMPT* model, however, includes normal mean maximum warmest month temperature in its accounting for the urban heat island effect because addressing the mean extreme is, generally, more attainable than addressing the extreme of extremes. Moreover, addressing the mean extreme, as opposed to the extreme of extremes, may often be considered to be a more efficient use of resources. Indeed, it may be better to plan for the mean extreme, which represents conditions that are more likely to happen on an annual basis, than conditions that are less likely to occur at a given time (n.b., to borrow from the example of flood hazard mitigation, it is noted that the United States Federal Emergency Management Agency [FEMA] requires that levees be designed to provide protection for floods that have a 1.0 percent chance of occurring on an annual basis [i.e., a 100-year flood], as opposed to a more extreme flood that has a 0.2 percent chance of occurring on an annual basis [i.e., a 500-year flood]). Please note, however, that this approach of planning for the mean extreme and not the extreme of extremes may not be universally applicable within the realm of hazard mitigation and climate change adaptation; it should not be applied without careful consideration outside of the context of application of the *UHIMPT* model.
2. As noted, the canopy layer urban heat island generally exhibits its highest amplitude during the nighttime hours. Although the data used to calculate the baseline measurements of urban heat island amplitude are not specifically representative of nighttime, the *UHIMPT* model, as explained in Section 2.2.2, uses urban heat island amplitude to develop estimates of mean warmest month and mean maximum warmest month air temperature within the urban heat island. Thus, the overall focus of the *UHIMPT* model is not on the mere amplitude, but on the total temperature to which the urban heat island amplitude contributes. Nonetheless, we note that while the canopy layer urban heat island generally exhibits its highest amplitude at nighttime, nighttime does not correspond to the highest air temperatures. This distinction is important given the *UHIMPT* model's incorporation of heat-related mortality. By developing an estimate of mean maximum warmest month air temperature within the urban

- heat island, however the basis for analysis of the maximum impacts of the urban heat island on heat-related mortality is provided.
3. Although the *UHIMPT* model makes use of a population size–urban heat island amplitude function for North American settlements, it can be easily adapted to incorporate similar functions for other regions.
  4. Despite its age, the population size–urban heat island amplitude function for North American settlements of Oke [34] remains the most comprehensive analysis of the relationship between population size and urban heat island amplitude of North American cities available to date. Moreover, it relies on a methodology that has been proven to be highly reliable in several subsequent studies (see: [39–41]).
  5. In the event that population should decline between two consecutive time steps, the factor of change in urban heat island amplitude is assumed to be zero. This assumes that no significant changes in urban geometry that would alter urban heat island amplitude accompany such a decline in population.
  6. A key explanation why the *UHIMPT* model uses an adaptation of Oke’s [34] population size–urban heat island amplitude function is to keep the model as simple as possible. Adding sky view factor measurements would result in the need to include their measurement, which would result in a significant increase in data input requirements for the user. However, as is indicated in Section 2.1.1, the *UHIMPT* model already includes a cohort-component population projection. By using an adaptation of Oke’s [34] population size–urban heat island amplitude function, the numbers of individual components and required inputs is reduced, which, thereby, simplifies the model and makes it more user-friendly and easier to run.
  7. Although sky view factor, which is directly representative of urban geometry, may, upon first consideration, seem to have a more direct relationship with the formation of the urban heat island effect than population size, population size is a reliable indicator of urban heat island amplitude when its relationship with temperature is determined at the regional level (see: [34,39,40]). By doing so, the influence of regional practices in land use and the construction and operation of the built environment, which impact urban heat island formation, are captured.
  8. Although long-term climate projections are generally reported as averages over multiple-year periods in order to reduce associated variability, the user-input projections are annualized in the *UHIMPT* model through the application of linear interpolation. This is done in order to make the projections of mean and mean maximum air temperatures compatible with the annual time step of the *UHIMPT* model.
  9. Please note that although the cohort-component population projection is used in, and impacts, the heat-related mortality calculations that are discussed in Section 2.1.1, it is not impacted by said calculations. The reason for this is associated with the fact that the *UHIMPT* model operates on an annual time step to simulate conditions in the warmest month. For the impacts of air temperature on population development to be isolated and reliably estimated on a continuous basis, the model would need to operate on a daily time step. However, given the presence of seasonal variability and the impacts of climate change, development of such a model that would simulate change over a continuous period (i.e., a period represented by a daily time step over multiple years) is impractical.
  10. It is important to note that mean summer and winter air temperatures, not mean maximum summer and mean minimum winter air temperatures (i.e., not extremes), are used to determine the appropriate relative risk factor for a given location. The reason for this is that the human capacity for acclimatization to higher temperatures is linked to climate as a whole, not just its extremes (see: [50,72]). Moreover, the temperature–mortality and temperature increase–acclimatization functions of Nordio et al. [50] have been developed with data that represents mean air temperatures. Nonetheless, as is described in Section 2.2, the impact of heat-related mortality on population dynamics is estimated using mean maximum warmest month air temper-

- atures. This allows the user to understand the impacts of extreme heat, as represented by projected mean maximum warmest month air temperatures.
11. Similar datasets based on the methodologies presented in Wang et al. [56] exist for Europe and Latin America and the Caribbean (see: [73,74]). It is recommended that the spatial resolution of alternate datasets be no less than 1.0 km<sup>2</sup>.
  12. Please note that Equations (3) and (4) include a modification of the population size–urban heat island amplitude function for North American settlements of Oke [34]. The original function was expressed by Oke [34] as:  $\Delta T_{u-r(max)} = 2.96 \log P - 6.41$ , where  $\Delta T_{u-r(max)}$  represents maximum urban heat island amplitude and  $P$  represents total population. The coefficient of determination of this function ( $r^2$ ), as calculated by Oke [34], was 0.96 (i.e.,  $r^2 = 0.96$ ).
  13. The constant (i.e., intercept) of the customized multiple linear regression model is excluded from Equations (5) and (6), and replaced with the mean and mean maximum urban heat island amplitude of the warmest month in a given time step (i.e.,  $\bar{A}_{x_{Warmest\ Month}}$  and  $\bar{A}_{x,Maximum_{Warmest\ Month}}$ , respectively). This is explained by the fact that the customized multiple linear regression model is used for no other purpose than to simulate the impacts of changes in surface albedo, impervious surface cover and the proportion of vegetation on urban heat island amplitude. While the constant (i.e., intercept) could be used, the UHIMPT model already includes a more-accurate simulation of urban heat island amplitude with  $\bar{A}_{x_{Warmest\ Month}}$  and  $\bar{A}_{x,Maximum_{Warmest\ Month}}$ . The acceptability of this adaptation is confirmed by the fact that the relative impacts of the independent variables remain unmodified.
  14. The linear regression model of Gallo et al. [30] is based on a comparison of air temperature and land surface temperature data, which was collected at a total of 14 United States Climate Reference Network meteorological observation stations located throughout the continental United States. Their model indicates that air temperature is a significant factor in explaining variation of land surface temperature ( $N = 14$ ;  $\beta = 1.15$ ;  $p = 0.01$ ). Their model, the coefficient of determination ( $r^2$ ) of which is 0.88, expresses the relationship between land surface temperature and air temperature as  $T_{Land} = 2.82 + (1.15 \times T_{Air})$ , where  $T_{Land}$  represents land surface temperature and  $T_{Air}$  represents air temperature. For use in Equations (5) and (6) of the UHIMPT model, which pertain to the modification of mean and mean maximum warmest month urban heat island amplitude, the linear regression model of Gallo et al. [30] has been algebraically restated as:  $T_{Air} = \frac{T_{Land} - 2.82}{1.15}$ . As restated, however, even a null value for  $T_{Land}$  will result in a value for  $T_{Air}$  that is not zero, but  $-2.452$ . This is problematic because the linear regression model is only used to convert the simulated impacts of alterations of surface albedo, impervious surface cover and the proportion of vegetation on land surface temperature to air temperature and lack of alteration would not result in change. Thus, application of a correction factor of 2.452 is necessary to cause a null value for  $T_{Land}$  to result in a value of zero for  $T_{Air}$ .
  15. Please note that change in  $\bar{I}$  is measured from negative one (i.e.,  $-1.0$ ) to one with one being the highest possible value. Negative values represent decreases in the proportion of impervious surface cover, which serves to mitigate the urban heat island effect. Positive values represent increases to the proportion of impervious surface cover, which increases the intensity of the urban heat island effect and is, therefore, undesirable in this instance. The value of change applied must be no more than the greatest possible positive or negative value less (i.e., minus) the initial (i.e., baseline) value.
  16. Please note that change in  $\bar{V}$  is measured from zero to one with one being the highest possible value. The value of change applied must be no more than the highest possible value less (i.e., minus) the initial (i.e., baseline) value.
  17. Please note that change in  $\bar{\alpha}$  is measured from zero to one with one being the highest possible value. The value of change applied must be no more than the highest possible value less (i.e., minus) the initial (i.e., baseline) value.

18. It is noted that this methodology results in the realization of projected temperatures at the midpoint of the projected period. This is supported by the fact that climate projections are typically reported as average values for multi-year periods (n.b., the aforementioned projections of Wang et al. [56] are reported as average values for 30-year periods). The realization of projected temperatures at the midpoint of the projected period facilitates an accurate portrayal of same because the midpoint is equivalent to the average between two or more points (e.g., starting point, ending point).
19. Equations (26)–(33) have been obtained through analysis of Figure 2, Part A of Nordio et al. [50] with the open-source graph digitizing software package known as Engauge Digitizer (Release 10.3) by Mark Mitchell of Torrance, California. Because of the method through which these equations have been obtained, they may differ slightly from those represented by the data used by Nordio et al. [50] to create aforesaid Figure 2, Part A. Analysis with Engauge Digitizer was necessary because Nordio et al. [50] report neither the data used to prepare the aforementioned figure, nor provide equations for the curves it represents. In Equations (26)–(33), curves are represented with sextic polynomial equations. This type of equation was chosen because it most accurately reflects all of the data represented in Figure 2, Part A of Nordio et al. [50]. The coefficient of determination ( $r^2$ ) for these equations ranges from 0.99970 in Equation (28) to 0.99995 in Equation (30).
20. As has been previously indicated, the parameterization of this component is based on the analysis of Nordio et al. [50], which indicates that every 5 °C increase in mean air temperature results in a 1.78 percent reduction in heat-related mortality. The *UHIMPT* model, however, applies this function continuously, such that every fractional degree increase in mean air temperature results in a corresponding percent reduction in heat-related mortality. In addition, as may be seen in Equation (37) this function is also applied bi-directionally, such that a decrease in mean temperature would result in a corresponding increase in the factor of relative risk of mortality. This results from the fact that subtracting a negative number results in adding a positive (e.g.:  $-5 - [-3] = -5 + 3 = -2$ ). Nevertheless, it is noted that, as may be seen in Equation (36), the acclimatization factor can only be negative if there is a decline in mean temperature between the current time step and the next time step. Given the general trend to higher mean temperatures as a result of global warming, a negative acclimatization factor is unlikely and only possible in the *UHIMPT* model if a decrease in mean temperature is indicated by the user-input mean temperature projections that have been described in Section 2.1.2.
21. Data representing areas that were at least partially located within a water feature were not entered into the multiple linear regression model. It is noted that the surface albedo and surface temperature of water features is generally low. However, low surface albedo over land is generally associated with high surface temperature. Data representing areas that were at least partially within a water feature were, therefore, excluded in order to prevent surface albedo over water from skewing the multiple linear regression model's depiction of the correlation between land surface temperature and surface albedo.
22. Had a modified cohort-component projection been applied in the *UHIMPT* model, a buildout analysis would have been required in order to estimate remaining development capacity. This would have dramatically increased user-input data requirements and model complexity, thereby potentially rendering the model less useful.
23. Despite its age, Oke's [34] population size–urban heat island amplitude function was used in the *UHIMPT* model because of its comprehensiveness, very high coefficient of determination (n.b., the coefficient of determination [ $r^2$ ] was 0.96 [i.e.,  $r^2 = 0.96$ ]), and the fact that no suitable alternative currently exists for the entirety of North America.
24. When calculating the sum of absolute differences between user-input mean summer and winter air temperatures and those of the climate clusters as provided by Nordio

et al. [50] in accordance with Equation (34), the difference between the climate cluster associated with the temperature–mortality function identified by the *UHIMPT* model’s approach and the climate cluster provided by Nordio et al. [50] was between 0.03 and 0.73, with a mean difference of 0.49, in eight of 48 cases.

25. It is noted that the raw data used by Nordio et al. [50] were unavailable in these tests. Had the mean summer and winter temperatures used by Nordio et al. [50] been available, it is likely that the accuracy of the *UHIMPT* model’s approach to selection of the appropriate temperature–mortality function would have been shown to be higher than demonstrated here. This is suggested by the fact that, when calculating the sum of absolute differences between user-input mean summer and winter air temperatures and those of the climate clusters as provided by Nordio et al. [50] in accordance with Equation (34), the difference between the climate cluster associated with the temperature–mortality function identified by the *UHIMPT* model’s approach and the climate cluster provided by Nordio et al. [50] was 0.73 or less in eight of 48 cases.

**Supplementary Materials:** The following are available online at <https://www.mdpi.com/2413-8851/5/1/19/s1>, Supplement A—Inventory of Data Input Requirements of *UHIMPT* Model; Supplement B—Development of Multiple Linear Regression Model Used in Equations (5) and (6); Supplement C—Philadelphia-Specific Data Inputs to Demonstrative *UHIMPT* Model; and Supplement D—Demonstrative *UHIMPT* Model in STELLA (.STMX) File Format. References [75–82] are cited in the supplementary materials.

**Funding:** This research received no external funding.

**Acknowledgments:** The author thanks Post-Retirement Professor David Brown (McGill University, School of Urban Planning) and Assistant Professor Ehab Diab (University of Saskatchewan, Department of Geography and Planning) for their comments and feedback on an initial draft of this article, as well as Professor Lisa Bornstein (McGill University, School of Urban Planning) for general support and guidance in model conceptualization. The author also thanks Luke Helsel, MS (Private Affiliation) and Andreas Schmidt (Private Affiliation) for their assistance in reviewing some of the equations presented in this article.

**Conflicts of Interest:** The author declares no conflict of interest.

## References

1. Kalkstein, L.; Greene, S.; Mills, D.; Samenow, J. An evaluation of the progress in reducing heat-related human mortality in major US cities. *Nat. Hazards* **2011**, *56*, 113–129. [[CrossRef](#)]
2. Cheng, C.; Campbell, M.; Li, Q.; Li, G.; Auld, H.; Day, N.; Pengelly, D.; Gingrich, S.; Klaasen, J.; MacIver, D.; et al. Differential and combined impacts of extreme temperatures and air pollution on human mortality in South-Central Canada. Part II: Future estimates. *Air Qual. Atmos. Health* **2009**, *1*, 223–235. [[CrossRef](#)]
3. Guest, C.; Wilson, K.; Woodward, A.; Henessy, K.; Kalkstein, L.; Skinner, C.; McMichael, A. Climate and mortality in Australia: Retrospective study, 1979–1990, and predicted impacts in five major cities in 2030. *Clim. Res.* **1999**, *13*, 1–15. [[CrossRef](#)]
4. Changnon, S.; Kunkel, K.; Reinke, B. Impacts and responses to the 1995 heatwave: A call to action. *Bull. Am. Meteorol. Soc.* **1996**, *77*, 1497–1506. [[CrossRef](#)]
5. Robine, J.-M.; Cheung, S.L.K.; Le Roy, S.; Van Oyen, H.; Griffiths, C.; Michel, J.-P.; Herrmann, F.R. Death toll exceeded 70,000 in Europe during the summer of 2003. *Comptes Rendus Biol.* **2008**, *331*, 171–178. [[CrossRef](#)] [[PubMed](#)]
6. Barriopedro, D.; Fischer, E.; Luterbacher, J.; Trigo, R.; Garcia-Herrera, R. The hot summer of 2010: Redrawing the temperature record map of Europe. *Science* **2011**, *332*, 220–224. [[CrossRef](#)] [[PubMed](#)]
7. Armstrong, B. *Estimated Number of Premature Deaths Attributable to Heat in England, 6–14 July 2013*; London School of Hygiene and Tropical Medicine: London, UK, 2013.
8. Shaposhnikov, D.; Revich, B.; Bellander, T.; Bedada, G.B.; Bottai, M.; Kharkova, T.; Kvasha, E.; Lezina, E.; Lind, T.; Semutnikova, E.; et al. Mortality related to air pollution with the Moscow heatwave and wildfire of 2010. *Epidemiology* **2014**, *25*, 359–364. [[CrossRef](#)] [[PubMed](#)]
9. IPCC. *Climate Change 2013: The Physical Science Basis, Contribution of Working Group I to the 5th Assessment Report of the Intergovernmental Panel on Climate Change*; Stocker, T.F., Qin, D., Plattner, G.-K., Tignor, M., Allen, S.K., Boschung, J., Nauels, A., Xia, Y., Bex, V., Midgley, P.M., Eds.; Cambridge University Press: Cambridge, UK, 2013.
10. He, W.; Goodkind, D.; Kowal, P. *An Aging World: 2015*; United States Government Publishing Office: Washington, DC, USA, 2016.

11. Frumkin, H. Urban sprawl and public health. *Public Health Rep.* **2002**, *117*, 201–217. [[CrossRef](#)]
12. Naughton, M.; Henderson, A.; Mirabelli, M.; Kaiser, R.; Wilhelm, J.; Kieszak, S.; Rubin, C.; McGeehin, M. Heat-related mortality during a 1999 heat wave in Chicago. *Am. J. Prev. Med.* **2002**, *22*, 221–227. [[CrossRef](#)]
13. Lugo-Amador, N.; Rothenhaus, T.; Moyer, P. Heat-related illness. *Emerg. Med. Clin. N. Am.* **2004**, *22*, 315–327. [[CrossRef](#)]
14. Harlan, S.; Brazel, A.; Prashad, L.; Stefanov, W.; Larsen, L. Neighborhood microclimates and vulnerability to heat stress. *Soc. Sci. Med.* **2006**, *63*, 2847–2863. [[CrossRef](#)] [[PubMed](#)]
15. Bouchama, A.; Dehbi, M.; Mohamed, G.; Mattheis, F.; Shoukri, M.; Menne, B. Prognostic factors in heat wave-related deaths: A meta-analysis. *Arch. Intern. Med.* **2007**, *167*, 2170–2176. [[CrossRef](#)] [[PubMed](#)]
16. Harlan, S.; Decket-Barreto, J.; Stefanov, W.; Petitti, D. Neighborhood effects on heat deaths: Social and environmental predictors of vulnerability in Maricopa County, Arizona. *Environ. Health Perspect.* **2013**, *121*, 197–204. [[CrossRef](#)] [[PubMed](#)]
17. Keller, R. *Fatal Isolation: The Devastating Paris Heat Wave of 2003*; University of Chicago Press: Chicago, IL, USA, 2015.
18. Kalkstein, L.; Greene, J.S. An evaluation of climate/mortality relationships in large US cities and the possible impacts of a climate change. *Environ. Health Perspect.* **1997**, *105*, 84–93. [[CrossRef](#)] [[PubMed](#)]
19. Doyon, B.; Bélanger, D.; Gosselin, P. The potential impact of climate change on annual and seasonal mortality for three cities in Québec, Canada. *Int. J. Health Geogr.* **2008**, *7*, 23–35. [[CrossRef](#)] [[PubMed](#)]
20. Hayhoe, K.; Sheridan, S.; Kalkstein, L.; Greene, S. Climate change, heatwaves, and mortality projections for Chicago. *J. Great Lakes Res.* **2010**, *36*, 65–73. [[CrossRef](#)]
21. Hajat, S.; Vardoulakis, S.; Heaviside, C.; Eggen, B. Climate change effects on human health: Projections of temperature-related mortality for the United Kingdom during the 2020s, 2050s and 2080s. *J. Epidemiol. Community Health* **2014**, *68*, 641–648. [[CrossRef](#)]
22. Kingsley, S.; Eliot, M.; Gold, J.; Vanderslice, R.; Wellenius, G. Current and projected heat-related morbidity and mortality in Rhode Island. *Environ. Health Perspect.* **2016**, *124*, 460–467. [[CrossRef](#)]
23. Li, T.; Horton, R.; Bader, D.; Zhou, M.; Liang, X.; Ban, J.; Sun, Q.; Kinney, P. Aging will amplify the heat-related mortality risk under a changing climate: Projection for the elderly in Beijing, China. *Sci. Rep.* **2016**, *6*, 28161. [[CrossRef](#)]
24. Huang, C.; Barnett, A.; Wang, X.; Vaneckova, P.; Fitzgerald, G.; Tong, S. Projecting future heat-related mortality under climate change scenarios: A systematic review. *Environ. Health Perspect.* **2011**, *119*, 1681–1690. [[CrossRef](#)]
25. Hémon, D.; Jougl, E. *Surmortalité liée à la canicule d'août 2003*; Institut national de la santé et de la recherche médicale: Paris, France, 2003.
26. Stone, B. *The City and the Coming Climate: Climate Change in the Places We Live*; Cambridge University Press: New York, NY, USA, 2012.
27. Roth, M. Urban heat islands. In *Handbook of Environmental Fluid Dynamics: Systems, Pollution, Modeling and Measurements*; Fernando, H., Ed.; CRC Press: Boca Raton, FL, USA, 2013; pp. 143–159.
28. Saaroni, H.; Ben-Dor, E.; Bitan, A.; Potchter, O. Spatial distribution and microscale characteristics of the urban heat island in Tel-Aviv, Israel. *Landsc. Urban Plan.* **2000**, *48*, 1–18. [[CrossRef](#)]
29. Martin, P.; Baudouin, Y.; Gachon, P. An alternative method to characterize the surface urban heat island. *Int. J. Biometeorol.* **2015**, *59*, 849–861. [[CrossRef](#)] [[PubMed](#)]
30. Gallo, K.; Hale, R.; Tarpley, D.; Yu, Y. Evaluation of the relationship between air and land surface temperature under clear and cloudy sky conditions. *J. Appl. Meteorol. Climatol.* **2011**, *50*, 767–775. [[CrossRef](#)]
31. Klok, L.; Zwart, S.; Verhagen, H.; Mauri, E. The surface heat island of Rotterdam and its relationship with urban surface characteristics. *Resour. Conserv. Recycl.* **2012**, *64*, 23–29. [[CrossRef](#)]
32. Dare, R. A review of local-level land use planning and design policy for urban heat island mitigation. *J. Extrem. Events* **2020**, *6*, 1–27. [[CrossRef](#)]
33. Bonan, G. *Ecological Climatology: Concepts and Applications*; Cambridge University Press: Cambridge, UK, 2008.
34. Oke, T. City size and the urban heat island. *Atmos. Environ.* **1973**, *7*, 769–779. [[CrossRef](#)]
35. Landsberg, H. *The Urban Climate*; Academic Press: New York, NY, USA, 1981.
36. Gaffin, S.; Rosenzweig, C.; Khanbilvardi, R.; Parshall, L.; Mahani, S.; Glickman, H.; Goldberg, R.; Blake, R.; Slosberg, R.; Hillel, D. Variations in New York City's urban heat island strength over time and space. *Theor. Appl. Climatol.* **2008**, *94*, 1–11. [[CrossRef](#)]
37. Miller, J. Urban and regional temperature trends in Las Vegas and southern Nevada. *J. Ariz. Nev. Acad. Sci.* **2011**, *43*, 27–39. [[CrossRef](#)]
38. László, E.; Bottyán, Z.; Szegedi, S. Long-term changes of meteorological conditions of urban heat island development in the region of Debrecen, Hungary. *Theor. Appl. Climatol.* **2016**, *124*, 365–373. [[CrossRef](#)]
39. Sakakibara, Y.; Matsui, E. Relation between heat island intensity and city size indices/urban canopy characteristics in settlements of Nagano Basin, Japan. *Geogr. Rev. Jpn.* **2005**, *78*, 812–824. [[CrossRef](#)]
40. Saaroni, H.; Ziv, B. Estimating the urban heat island contribution to urban and rural air temperature differences over complex terrain: Application to an arid city. *J. Appl. Meteorol. Climatol.* **2010**, *49*, 2159–2166. [[CrossRef](#)]
41. Huang, Q.; Lu, Y. The effect of urban heat island on climate warming in the Yangtze River delta urban agglomeration in China. *Int. J. Environ. Res. Public Health* **2015**, *12*, 8773–8789. [[CrossRef](#)]
42. Oke, T. Canyon geometry and the nocturnal urban heat island: Comparison of scale model and field observations. *J. Climatol.* **1981**, *1*, 237–254. [[CrossRef](#)]

43. Svensson, M. Sky view factor analysis: Implications for urban air temperature differences. *Meteorol. Appl.* **2004**, *11*, 201–211. [[CrossRef](#)]
44. Blankenstein, S.; Kuttler, W. Impact of street geometry on downward longwave radiation and air temperature in an urban environment. *Meteorol. Z.* **2004**, *13*, 373–379. [[CrossRef](#)]
45. Shryock, H.; Siegel, J.; Larmon, E.; Bayo, F.; Davidson, M.; Demeny, P.; Glick, P.; Grabill, W.; Grove, R.; Israel, R.; et al. *The Methods and Materials of Demography*; United States Census Bureau: Washington, DC, USA, 1975.
46. Klosterman, R. *Community Analysis and Planning Techniques*; Rowman and Littlefield Publishers: Lanham, MD, USA, 1990.
47. Smith, S.; Tayman, J.; Swanson, D. *State and Local Population Projections: Methodology and Analysis*; Kluwer Academic Publishers: New York, NY, USA, 2002.
48. Berke, P.; Godschalk, D.; Kaiser, E.; Rodriguez, D. *Urban Land Use Planning*; University of Illinois Press: Urbana, IL, USA, 2006.
49. Swanson, D.; Tayman, J. *Subnational Population Estimates*; Springer: Dordrecht, The Netherlands, 2012.
50. Nordio, F.; Zanutti, A.; Colicino, E.; Kloog, I.; Schwartz, J. Changing patterns of the temperature–mortality association by time and location in the United States, and implications for climate change. *Environ. Int.* **2015**, *81*, 80–86. [[CrossRef](#)]
51. Day, J. *Population Projections of the United States by Age, Sex, Race, and Hispanic Origin: 1995 to 2050*; United States Census Bureau: Washington, DC, USA, 1996.
52. Treadway, R. *Population Projections for the State and Counties of Illinois*; Springfield: Geneseo, IL, USA, 1997.
53. Curriero, F.; Heiner, K.; Samet, J.; Zeger, S.; Strug, L.; Patz, J. Temperature and mortality in 11 cities of the eastern United States. *Am. J. Epidemiol.* **2002**, *156*, 80–87. [[CrossRef](#)]
54. Bai, L.; Ding, D.; Gu, S.; Bi, P.; Su, B.; Qin, D.; Xu, G.; Liu, Q. The effects of summer temperature and heat waves on heat-related illness in a coastal city of China, 2011–2013. *Environ. Res.* **2014**, *132*, 212–219. [[CrossRef](#)]
55. Bobb, J.; Peng, R.; Bell, M.; Dominici, F. Heat-related mortality and adaptation to heat in the United States. *Environ. Health Perspect.* **2014**, *122*, 811–816. [[CrossRef](#)]
56. Wang, T.; Hamann, A.; Spittlehouse, D.; Carroll, C. Locally downscaled and spatially customizable climate data for historical and future periods for North America. *PLoS ONE* **2016**, *11*, e0156720. [[CrossRef](#)]
57. Forrester, J.; Senge, P. Tests for building confidence in system dynamics models. In *TIMS Studies in the Management Sciences*; Legasto, A., Forrester, J., Lyneis, J., Eds.; North Holland Publishing Company: Amsterdam, The Netherlands, 1980; Volume 14, pp. 209–228.
58. Barlas, Y. Multiple tests for validation of system dynamics type of simulation models. *Eur. J. Oper. Res.* **1989**, *42*, 59–87. [[CrossRef](#)]
59. Qudrat-Ullah, H. On the validation of system dynamics type simulation models. In Proceedings of the International Conference on Information Science and Applications, Seoul, Korea, 21–23 April 2010.
60. Oke, T. The energetic basis of the urban heat island. *Q. J. R. Meteorol. Soc.* **1982**, *108*, 1–24. [[CrossRef](#)]
61. Grimmond, C.S.B.; Potter, S.; Zutter, H.; Souch, C. Rapid methods to estimate sky-view factors applied to urban areas. *Int. J. Climatol.* **2001**, *21*, 903–913. [[CrossRef](#)]
62. Guo, Y.; Gasparrini, A.; Armstrong, B.G.; Tawatsupa, B.; Tobias, A.; Lavigne, E.; De Sousa-Zanotti-Stagliorio-Coelho, M.; Pan, E.; Kim, H.; Hashizume, M.; et al. Heat wave and mortality: A multicounty, multicomunity study. *Environ. Health Perspect.* **2017**, *125*, 087006. [[CrossRef](#)] [[PubMed](#)]
63. Anderson, B.; Bell, M. Heat waves in the United States: Mortality risk during heat waves and effect modification by heat wave characteristics in 43 United States communities. *Environ. Health Perspect.* **2011**, *119*, 210–218. [[CrossRef](#)]
64. Basagaña, X.; Sartini, C.; Barrera-Gómez, J.; Dadvand, P.; Cunillera, J.; Ostro, B.; Sunyer, J.; Medina-Ramón, M. Heat waves and cause-specific mortality at all ages. *Epidemiology* **2011**, *22*, 765–772. [[CrossRef](#)] [[PubMed](#)]
65. Schuman, S. Patterns of urban heat-wave deaths and implications for prevention: Data from New York and St. Louis during July 1966. *Environ. Res.* **1972**, *5*, 59–75. [[CrossRef](#)]
66. Hajat, S.; Kovats, R.; Atkinson, R.; Haines, A. Impact of hot temperatures on death in London: A time series approach. *J. Epidemiol. Community Health* **2002**, *56*, 367–372. [[CrossRef](#)]
67. Joe, L.; Hoshiko, S.; Dobraca, D.; Jackson, R.; Smorodinsky, S.; Smith, D.; Harnly, M. Mortality during a large-scale heat wave by place, demographic group, internal and external causes of death, and building climate zone. *Int. J. Environ. Res. Public Health* **2016**, *13*, 299–315. [[CrossRef](#)]
68. Schilling, J.; Logan, J. Greening the rust belt: A green infrastructure model for right sizing America’s shrinking cities. *J. Am. Plan. Assoc.* **2008**, *74*, 451–466. [[CrossRef](#)]
69. Bontje, M. Facing the challenge of shrinking cities in East Germany: The case of Leipzig. *GeoJournal* **2004**, *61*, 13–21. [[CrossRef](#)]
70. Fuhrich, M. Renaturierung als Vorwärtsstrategie nachhaltiger Stadtentwicklung. *Infor. Raumentwick.* **2009**, *7*, 503–514.
71. Bonham, B.; Smith, P. Transformation through greening. In *Growing Greener Cities: Urban Sustainability in the Twenty-First Century*; Birch, E., Wachter, S., Eds.; University of Pennsylvania Press: Philadelphia, PA, USA, 2008; pp. 227–243.
72. Honda, Y.; Ono, M.; Ebi, K.L. Adaptation to the heat-related health impact of climate change in Japan. In *Climate Change Adaptation in Developed Nations: From Theory to Practice*; Ford, J.D., Berrang-Ford, L., Eds.; Springer: Dordrecht, The Netherlands, 2011; pp. 189–203.
73. Hamman, A. ClimateEU: Historical and Projected Climate Data for Europe. Available online: <https://sites.ualberta.ca/~jahamann/data/climateeu.html> (accessed on 6 October 2017).

74. Hamman, A. ClimateSA: Historical and projected climate data for Mexico, Central and South America. Available online: <https://sites.ualberta.ca/~jahamann/data/climatesa.html> (accessed on 6 October 2017).
75. Rouse, J.; Haas, R.; Schell, J.; Deering, D. Monitoring vegetation systems in the great plains with ERTS. In Proceedings of the Third Earth Resources Technology Satellite Symposium, Washington, DC, USA, 10–14 December 1973.
76. Jiménez-Muñoz, J.; Sobrino, J.; Gillespie, A.; Sabol, D.; Gustafson, W. Improved land surface emissivities over agricultural areas using ASTER NDVI. *Remote Sens. Environ.* **2006**, *103*, 474–487. [[CrossRef](#)]
77. Avdan, U.; Jovanovska, G. Algorithm for automated mapping of land surface temperature using Landsat 8 satellite data. *J. Sens.* **2016**, *2016*, 1480307. [[CrossRef](#)]
78. United States Geological Survey (2017). Using the USGS Landsat 8 Product. Available online: <https://landsat.usgs.gov/using-usgs-landsat-8-product> (accessed on 14 November 2017).
79. Sobrino, J.; Jiménez-Muñoz, J.; Paolini, L. Land surface temperature retrieval from Landsat TM 5. *Remote Sens. Environ.* **2004**, *90*, 434–440. [[CrossRef](#)]
80. Yu, X.; Guo, X.; Wu, Z. Land surface temperature retrieval from Landsat 8 TIRS—Comparison between radiative transfer equation-based method, split window algorithm and single channel method. *Remote Sens.* **2014**, *6*, 9829–9852. [[CrossRef](#)]
81. Lee, D.; Seo, M.; Lee, K.-S.; Choi, S.; Sung, N.-H.; Kim, H.; Jin, D.; Kwon, C.; Huh, M.; Han, K.-S. Landsat 8-based high resolution surface broadband albedo retrieval. *Korean J. Remote Sens.* **2016**, *32*, 741–746. [[CrossRef](#)]
82. Xu, H. Modification of normalized difference water index (MNDWI) to enhance open water features in remotely sensed imagery. *Int. J. Remote Sens.* **2006**, *27*, 3025–3033. [[CrossRef](#)]